A reassessment of the postcanine dentition and systematics of the tritylodontid Stereognathus (Cynodontia, Tritylodontidae, Mammaliamorpha), from the Middle Jurassic of the UK

A reassessment of the postcanine dentition and systematics of the tritylodontid *Stereognathus* (Cynodontia, Tritylodontidae, Mammaliamorpha), from the Middle Jurassic of the UK

Journal:	*Journal of Vertebrate Paleontology*
Manuscript ID	JVP-2017-0033.R2
Manuscript Type:	Article
Date Submitted by the Author:	n/a
Complete List of Authors:	Panciroli, Elsa; University of Edinburgh School of GeoSciences, ; National Museum of Scotland, Walsh, Stig; National Museums Scotland, Natural Sciences Fraser, Nicholas; National Museums Scotland Brusatte, Stephen; University of Edinburgh School of GeoSciences Corfe, Ian; University of Helsinki, Institute of Biotechnology
Key Words:	Stereognathus, Tritylodontidae, Mammaliamorpha, Cynodontia, Middle Jurassic, Systematics

A reassessment of the postcanine dentition and systematics of the tritylodontid *Stereognathus* (Cynodontia, Tritylodontidae, Mammaliamorpha), from the Middle Jurassic of the UK

ELSA PANCIROLI, [*,1,2], STIG WALSH,[2] NICK FRASER, [2] STEPHEN L. BRUSATTE,[1,2] and IAN CORFE[3]

[1]School of Geosciences, University of Edinburgh, Grant Institute, Kings Buildings, Edinburgh EH9 3FE United Kingdom, elsa.panciroli@ed.ac.uk; s.brusatte@ed.ac.uk;

[2]National Museum of Scotland, Chambers St, Edinburgh EH1 1JF, United Kingdom, s.walsh@nms.ac.uk;

[3]Jernvall EvoDevo Lab, Institute of Biotechnology, University of Helsinki, P.O. Box 56, FIN-00014 Helsinki, Finland, ian.corfe@helsinki.fi

*Corresponding author

ABSTRACT—Tritylodontidae was a successful advanced cynodont clade with a close relationship to mammals, but falling outside the clade Mammaliaformes. *Stereognathus ooliticus* was the first tritylodontid to be named and described in 1854, but since then no comprehensive description for this species has been made. A second species, *S. hebridicus*, was named in 1972 and diagnosed based solely on size difference, being larger than the *S. ooliticus* holotype. We re-examined all postcanine tooth material attributed to the genus *Stereognathus* to test the species diagnosis and identify diagnostic morphological characters for this genus. We find no statistical difference in size distribution between *S. ooliticus* and *S. hebridicus* postcanine specimens. Specimens previously attributed to the different species fall along an ontogenetic spectrum of size, with no clear clustering. Morphologically, we affirm many previous described features for *Stereognathus*, and identify new morphological features in upper and lower postcanines. We find no morphological features to distinguish these two species, and therefore synonymize *S. hebridicus* under *S. ooliticus*. We re-evaluate the scoring of *S. ooliticus* in previous phylogenetic analyses, generating a new tree using rescored *Stereognathus* characters. Finally, we suggest similar re-evaluations and re-descriptions of other poorly described tritylodontid material is necessary to further clarify relationships among Tritylodontidae and the evolution of characters in derived genera such as *Stereognathus*.

INTRODUCTION

Tritylodontids are advanced cynodont mammaliamorphs that fall outside the clade Mammaliaformes, but their close relationship to mammals is now generally accepted (Rowe 1993; Luo *et al.,* 2002; Ruta et al., 2013). Superficially, tritylodontids would have appeared rodent-like: enlarged procumbent incisors replaced the absent canine teeth, they possessed a diastema, and their postcanine teeth were highly specialized for herbivory. Tritylodontids ranged in size from genera such as *Bocatherium*, at < 5 cm skull length (Clark and Hopson, 1985) up to larger genera with > 22 cm skull lengths, such as *Kayentatherium* (Kermack, 1982). They were the last surviving family of non-mammaliaform cynodonts, appearing in the fossil record in the Late Triassic (Hennig, 1922; Fedak et al., 2015), living alongside early mammals and other mammaliaforms throughout the Jurassic and persisting into the Early Cretaceous (Maisch et al., 2004; Hu et al., 2009; Matsuoka et al., 2016). Although they shared many cranial and postcranial features with early mammaliaformes, they retained a quadrate-articular jaw joint, lacking a dentary-squamosal contact, and they had a large angular process and coronoid process on the dentary (Kemp, 2005). Their size range, and specializations for herbivory, are among the characteristics that distinguish them from many of the early mammals they lived alongside (Kemp, 2005).

Tritylodontidae currently includes over seventeen genera (with at least five more genera debated or synonymized) and have been described from Africa (Owen

1884; Fourie, 1963), Antarctica (Lewis, 1986; Hammer and Smith 2008), Asia (Young, 1940, 1982; Chow and Hu, 1959; Cui, 1976, 1981; He and Cai, 1984; Luo and Sun, 1994; Matsuoka and Setoguchi, 2000; Maisch *et* al., 2004; Lopatin and Agadjanian 2008; Watabe et al., 2007; Hu et al., 2009; Matsuoka et al., 2016; Velazco et al., 2017), Europe (Charlesworth, 1854; Owen, 1857; Hennig, 1922; Waldman and Savage, 1972; Ensom, 1977, 1994), and North America (Kermack, 1982; Sues, 1985, 1986; Sues and Jenkins, 2006; Fedak et al., 2015), including Mexico (Clark and Hopson, 1985). All are considered herbivorous (Kühne, 1956; Sues, 1986), except *Yuanotherium minor* which was described as having dental characteristics that suggest it may have been omnivorous (Hu et al., 2009).

Stereognathus was the first tritylodontid genus named and identified (Charlesworth 1854). Since that time, material from across the UK has been assigned to *Stereognathus*, and its name appears regularly on faunal lists. However, the anatomy and taxonomy of this genus remain poorly understood. Two species have been described: the type species *S. ooliticus* (Charlesworth 1854) is currently represented by hundreds of cusp fragments, and at least 48 somewhat more complete postcanine teeth, two incisors, one edentulous fragment of maxilla, and the holotype comprising three postcanines in a fragment of maxilla. All of this material comes from sites in England (for overview see Evans and Milner, 1994). A second species, *S. hebridicus,* was named by Waldman and Savage (1972) from the Isle of Skye in Scotland. Fossils assigned to this species currently include 41 postcanines, many of them fragmentary and/or badly worn, with two in excellent condition and described herein. Although a few isolated limb bones have been collected from UK sites and assigned to Tritylodontidae - notably a single femur from the Stonesfield

slate (Simpson, 1928; Kühne, 1956) - the identification as *Stereognathus* remains unconfirmed. We therefore consider these specimens to be outside the scope of this study.

Surprisingly, given the long history and amount of fossil material, *Stereognathus* has yet to be comprehensively described. There is currently a lack of clarity on its diagnosis, systematics, anatomical features, and variability. This is becoming a pressing issue as new tritylodontid specimens continue to be discovered around the world (e.g., Matsuoka et al., 2016; Velazco et al., 2017), yet cannot easily be compared to *Stereognathus*. Lack of detailed descriptions of some genera have repercussions for phylogenetic analyses, including incorrect character scoring for *Stereognathus*. Without the establishment of a firm description and diagnosis for *Stereognathus*, this remains unclear. Finally, recent field work on the Isle of Skye is discovering new *Stereognathus* specimens at a steady pace. This material has raised questions regarding their taxonomy, given that the original diagnosis of *S. hebridicus* was based only on a proposed size difference with *S. ooliticus*.

Here, we provide a reassessment of the anatomy of the postcanine dentition of *Stereognathus*, based upon all available material from the UK. We redescribe the holotype of *S. ooliticus* and synonymize *S. hebridicus* with *S. ooliticus,* based on close examination of *S. hebridicus* material. This includes the holotype and paratypes, alongside new and exceptionally well preserved postcanines from the Isle of Skye. We test whether specimens assigned to *S. hebridicus* from Skye, are indeed statistically significantly larger than the English specimens, as stated in the original diagnosis of *S. hebridicus*. We discuss anatomical and size variation within the genus and provide a comprehensive anatomical description of *Stereognathus,*

identifying previously unrecognized morphology. We also run a phylogenetic analysis using new scorings based on these data, and discuss the implications of incomplete data on our understanding of tritylodontid phylogeny.

Institutional Abbreviations—**BGS**, British Geological Survey, UK; **BRSUG**, Geology Museum, University of Bristol, UK (formerly UBGM); **DORCM**, Dorset County Museum; **GLRCM**, Gloucester City Museum; **NHMUK**, Natural History Museum, London; **NMS**, National Museum of Scotland, UK; **OUMNH**, Oxford University Museum of Natural History.

Localities —*Stereognathus* material in the UK has so far exclusively been found in Bathonian (Middle Jurassic) limestones and mudstones in two regions: southern England and the Isle of Skye in Scotland. These localities are similar geologically: they generally represent coastally placed, mostly brackish lagoonal environments prone to drying out and subject to marine transgressions caused by subsidence and sea-level change. Some sites have more freshwater influx.

The oldest microvertebrate site to yield *Stereognathus* material is Hornsleasow Quarry, part of the Chipping Norton Limestone Formation: it is early Bathonian and is a Site of Special Scientific Interest (SSSI) because it preserves a complete succession of Sharp's Hill Beds (Metcalf et al., 1992). Material comes from a productive clay lens, likely formed in a fresh to brackish water small pond, within close distance of the coast (Metcalf et al. 1992). Finds include crocodylian teeth and osteoderms, turtle plates, and multiple fragmentary remains of small reptiles. There are also rarer pterosaur teeth and some small theropod and ornithischian dinosaur teeth, as well as a few larger remains such as *Cetiosaurus* teeth and bones, and

Megalosaurus teeth (Evans and Milner, 1994). Mammals and tritylodontids are present but appear less abundant than at other Bathonian microvertebrate localities, except the Taynton Limestone Formation (E. Panciroli pers. obs.; Evans and Milner, 1994).

The Stonesfield Slate is the informal, but still commonly used name for what is now the Taynton Limestone Formation in Oxfordshire. It is middle Bathonian, and comprises layers of thin oolite between fine grained calcareous sandstones (Sellwood and McKerrow, 1974). This estuarine assemblage contains an abundance of invertebrates and fish, alongside crocodilians and marine reptiles. Terrestrial material is less common. The Kilmaluag Formation on the Isle of Skye is also middle Bathonian in age, although exact biostratigraphical correlations with English sites have proven difficult (Barron et al*.,* 2012). It is part of the Middle Jurassic Great Estuarine Group of the Hebrides Basin. It comprises argillaceous limestones and calcareous mudstones formed in ephemeral lagoonal environments that periodically dried out, with marine horizons indicating basin subsidence and marine transgression (Hudson, 1980; Andrews, 1985; Barron et al., 2012).

Kirtlington Cement Quarry is a late Bathonian locality which has been especially productive for microvertebrates, yielding a similar assemblage to Hornsleasow (see above), but with many more mammal species and specimens recovered in more complete condition (Evans and Milner 1994), including tritylodontid material. The Mammal Bed is unconsolidated marly clay overlying a coral limestone, and the freshwater gastropods and ostracods within it suggest it represents a swampy habitat near the coast. Westcliff, also known as Watton Cliff, in

Dorset, is also a late Bathonian locality. It was an offshore bank in which terrestrial debris collected (Holloway, 1983).

Woodeaton has yielded material of both middle and late Bathonian age, with vertebrate material similar in composition to the other UK Bathonian microvertebrate locations (Evans and Milner, 1994; Parraga et al., 2016). Tritylodontid material has been recovered from this location from middle and late Bathonian horizons, and is morphologically indistinguishable from that recovered from the other UK sites (E. Panciroli pers. obs.). This material is currently being described by researchers at NHMUK (Parraga et al., 2016).

Tritylodontid material has also been identified in unprocessed samples from Tarlton Clay Pit, Leigh Delamere, and Swyre (all Bathonian, part of the Forest Marble), but is very fragmentary, comprising only a few single isolated cusps.

MATERIALS AND METHODS

Materials

We studied material assigned to *Stereognathus ooliticus* and *S. hebridicus*, as well as *Stereognathus* sp. and unspecified Tritylodontidae from the aforementioned UK localities. See Localities for details.

S. ooliticus material from BGS comprises the holotype BGS GSM113834, a fragment of maxilla with three postcanines collected from the Taynton Limestone Formation (Stonesfield Slate) in Oxfordshire, England. From DORCM specimens

G11048 and G10828, postcanines from the Forest Marble. From GLRCM specimens, MLR 20-22, MLR 20-38, GLRCM 10174, GLRCM 2104, GLRCM 2105_4, GLRCM 2105_6, GLRCM G50137, GLRCM G50236, GLRCM G50505, GLRCM G50506, GLRCM G50507, GLRCM G50508, GLRCM G50647, GLRCM G50705, GLRCM G50907, GLRCM G51108, GLRCM G51221, GLRCM G51222, GLRCM G51223, GLRCM G51224, GLRCM G51243, GLRCM G51244, GLRCM G51245, GLRCM G51520, GLRCM G51521, GLRCM G51616, GLRCM G51823, GLRCM G51906, GLRCM G51907, GLRCM G52021, GLRCM G52022, GLRCM G52026, GLRCM G52027, GLRCM G52038, GLRCM G52127, GLRCM G52202, GLRCM G52204, GLRCM G52205, GLRCM G52304, GLRCM G52641, GLRCM G52643, GLRCM G52820, GLRCM G52861, GLRCM G53402, GLRCM G53403, GLRCM G53404, GLRCM G53405, GLRCM G53406, GLRCM G53407, GLRCM G53408, GLRCM G53409, GLRCM G53410, GLRCM G53411, GLRCM G53412, GLRCM G53413, GLRCM G53414, GLRCM G53415, GLRCM G53416, GLRCM G53417, GLRCM G53418, GLRCM G53419, GLRCM G53420, GLRCM G53421, GLRCM G53422, GLRCM G53423, GLRCM G53424, GLRCM G53425, GLRCM G53426, GLRCM G53427, GLRCM G53428, GLRCM G53429, GLRCM G53430, GLRCM G53431, GLRCM G53432, GLRCM G53433, GLRCM G53434, GLRCM G53435, GLRCM G53804, GLRCM G53806, GLRCM G53807, GLRCM G53809, GLRCM G53811, GLRCM G53812, GLRCM G54017, GLRCM G54018, GLRCM G54610, GLRCM G54633, GLRCM G54634, GLRCM G54635, GLRCM G54701, GLRCM G54702, GLRCM G54703, GLRCM G54810, GLRCM G54811, GLRCM G55225, GLRCM G55226, GLRCM G55227, GLRCM G55534, GLRCM G55810, GLRCM G56416, GLRCM G56424, GLRCM G56425, GLRCM G56426, GLRCM

G56433, GLRCM G510202, GLRCM G510203, GLRCM G510204, GLRCM G510205, GLRCM G510206, GLRCM G510207, GLRCM G510208, GLRCM G510209, GLRCM G510210, GLRCM G510211 GLRCM G75710, which are all postcanines from Hornsleasow, mostly single cusps.

At the NHMUK the following postcanine fragments are identified as *S. ooliticus*: NHMUK PV M.36503, NHMUK PV M.36510, NHMUK PV M.36534, NHMUK PV M.36537, and NHMUK R.8720, and the following postcanine fragments are identified as Tritylodontidae - we identify them as *Stereognathus ooliticus*: NHMUK PV M.36534, NHMUK PV M.36539, NHMUK PV M.36506, NHMUK PV M.36543, NHMUK PV M.46103, NHMUK PV M.46266, NHMUK PV M.46261, NHMUK PV M.45265, NHMUK PV M.46268, NHMUK PV M.46270, NHMUK PV M.46271, NHMUK PV M.46273, NHMUK PV M.46274, NHMUK PV M.46272, NHMUK PV M.46374, NHMUK PV M.46375, NHMUK PV M.46277, NHMUK PV M.46373, NHMUK PV M.46382, NHMUK PV M.46383, NHMUK PV M.46384, NHMUK PV M.46386, NHMUK PV M.46403, NHMUK PV M.46415. The following are also identified as Tritylodontidae, but we do not identify them as tritylodontid: NHMUK PV M.46255 NHMUK PV M.46263. All of this material is from Kirtlington Cement Quarry, Oxfordshire, England, except NHMUK R.8720, which is from Westcliff.

At the OUMNH, specimen J.21790 is an edentulous fragment of *S.ooliticus* maxilla from the Taynton Limestone Formation (Stonesfield Slate) and the following postcanines (mostly fragmentary) are *Stereognathus* sp. from Kirtlington Cement Quarry, but we consider them all to be *S. ooliticus*: OUMNH J.79435, OUMNH J.79439, OUMNH J.79447, OUMNH J.79448, OUMNH J.79459, OUMNH J.79466,

OUMNH J.79469, OUMNH J.79470, OUMNH J.79471, OUMNH J.79477, OUMNH J.79478, OUMNH J.79480, OUMNH J.79484, OUMNH J.79492, and OUMNH J.21790.

BRSUG material comprises *Stereognathus hebridicus* postcanine material: holotype postcanine BRSUG 20572; paratypes BRSUG 20573, BRSUG 20574, BRSUG 20575; and more fragmentary specimens BRSUG 29000-29002 and BRSUG 28996-28999 (the latter specimen numbers include four to five postcanines grouped together per specimen number. All of this material was collected in the 1970s and 1980s near Elgol, from the Kilmaluag Formation, Middle Jurassic, Isle of Skye.

NMS material comprises dental remains of *Stereognathus hebridicus*: NMS G.1992.47.120 (comprising two specimens in same matrix) and NMS G.2017.17.6 collected in the 1980s, and NMS G.2017.17.1, NMS G.2017.17.2, NMS G.2017.17.3, NMS G.2017.17.4, and NMS G.2017.17.5 collected between 2013-2016 during fieldwork at various sites in the Kilmaluag Formation on the coast north of Elgol (Middle Jurassic, Isle of Skye). This includes some of the most intact postcanine material yet found, figured here for the first time.

Methods

Terminology—We use the cusp terminology modified from Watabe et al., (2007) with additions of the *pia* (posterior interlocking area) and *aia* (anterior interlocking area) from Lopatin and Agadjanian (2008) (Fig. 1). We adhere to the convention of referring to tritylodontid molars as ‘postcanines’, despite the absence of canines in tritylodontids. We use the cusp formula as begun by Simpson (1928),

specifying buccal, medial and lingual numbers of cusps, for example 2-2-2 in *Stereognathus*; that is, two cusps in each longitudinal row. Postcanine can be abbreviated to PC (uppers) or pc (lowers); likewise to indicate buccal, medial and lingual we use upper case for cusp terminology in the upper postcanines (B, M and L), and lower case for lower cusps (b, m, and l). There is debate over the homology of cusps between more basal tritylodontids (such as *Oligokyphus* which is considered the most basal tritylodontid), and derived tritylodontids such as *Stereognathus*, which have a reduced cusp number. Based on *Oligokyphus* being the most basal genus (Clark and Hopson, 1985; Setoguchi et al., 1999), it appears that cusp reduction in later tritylodontids may have taken place at the anterior of the upper postcanine, and posterior of the lower. This is suggested by the presence of vestigial cusps at these loci. Therefore the posteriormost upper medial and lingual cusps are M3 and L3, and lower the anteriormost cusps are b1 m1 and l1. Previous authors have considered the posteriormost buccal cusp in the upper molar as B2, not B3. While we adhere to this convention, the homology of these cusps requires further study. We consider in-depth discussions of which cusps are present, absent or vestigial from the ancestral condition to be outside the scope of this study. For more information see discussions in Watabe et al., (2007) and Matsuoka et al., (2016).

Measurements—Measurements were taken with electronic digital callipers where possible. For specimens still in matrix, measurements were taken from digitally reconstructed microCT scans in Mimics 19.0. All microCT scans were digitally reconstructed and image processed using Mimics 19.0 at the National Museum of Scotland. Specimens were also observed using conventional

microscopy, and morphological features recorded qualitatively based on previous literature and our observations. Maximum length and width were taken. To produce a large enough sample for statistical analysis, where minimal portions of a tooth were missing or worn, a conservative estimate of the original size was made, based on the proportions of more complete specimens.

Specimen Preparation—Specimen NMS G.1992.47.120 was prepared by coating them in paraloid B72 then using 10% acetone to remove the surrounding limestone matrix. When the tooth became too fragile to continue this process, micro-computed tomographic data were obtained using the µCT scanner built in-house at the University of Edinburgh, School of Geosciences Experimental Geoscience Facility. The scanner comprises a Feinfocus 10-160kV dual transmission/reflection source, MICOS UPR-160-AIR ultra-high precision air-bearing table, Perkin Elmer XRD0822 amorphous silicon x-ray flat panel detector and terbium doped gadolinium oxy-sulfide scintillator. An 0.8 mm aluminium plate limited beam hardening, and data were acquired using a reflection source with a peak energy of 120kV and 10W target power. Data acquisition software was written in-house, and scans were reconstructed using Octopus 8.7 software. The holotype of *S. ooliticus* BGS GSM113834 was also scanned in-house at Edinburgh, using a 1.6 mm aluminium plate. Historic specimens from BRSUG were mechanically prepared in the 1970s and 1980s. The *S. hebridicus* holotype 20572, and paratypes 20573, 20574, 20575, were µCT scanned at the University of Bristol using a Nikon XTH225ST scanner with a 225kV rotating target with a peak energy of kV140.

Phylogenetic Analysis—Trees were analysed using TNT version 1.5 (Goloboff, 2008), and the character matrix of 35 characters and 17 taxa is based on

Velazco et al. (2017), with *Stereognathus* rescored to reflect our findings (Appendix 1-2). We used the New Technology search, selecting ratchet, sectorial search, tree drift and tree fusing. The character states were unordered, and *Oligokyphus* was used as the outgroup as it is considered the most basal tritylodontid (Clark and Hopson, 1985; Setoguchi et al., 1999).

SYSTEMATIC PALAEONTOLOGY

SYNAPSIDA Osborn, 1903

CYNODONTIA Owen, 1861

MAMMALIAMORPHA Rowe, 1988

TRITYLODONTIDAE Cope, 1884

STEREOGNATHUS Charlesworth, 1854

STEREOGNATHUS OOLITICUS Charlesworth, 1854

STEREOGNATHUS HEBRIDICUS Waldman and Savage, 1972:120-122, fig. 1 (original description)

Holotype—BGS GSM113834, fragment of left maxilla with three postcanines and four empty postcanine sockets. Collected from the Stonesfield Slate (now Taynton Limestone Formation), Oxfordshire (see Localities).

Etymology—Named *ooliticus* for the Great Oolite Group, the contemporary name for the geological formation from which it was first described.

Revised Diagnosis—postcanines are quadrate in shape, rhomboidal in occlusal view, with cusp formula PC 2-2-2/pc 2-2. Cusps are subequal in size, with cusps longitudinally displaced anterioposteriorly. Intercuspal grooves are deep and v-shaped, and medial ridges of the cusps meet in the intercuspal-groove subequally in unworn teeth. In upper postcanines the ridges of L/M3 and B2 embrace the base of cusps L/M2 and B1. There are cuspules posterior and lingual to cusp L2, and sometimes B1. In the upper postcanines, vestigial cusps are found anterior to each longitudinal row of cusps, forming part of the *aia*. The *aia* extends across the anterior edge of the tooth bucco-lingually in the upper PCs, and the *pia* forms a bucco-lingual projection on the posterior edge of the tooth. Upper PCs have six to seven roots.

In lower pcs the *aia* forms a bucco-lingual projection and the *pia* comprises two embayments, the latter ridged inside and containing vestigial cusps l/b3. The *pia* is framed by the posterobuccal and posterolingual terminations of the b2 and l2 cusp ridges, and separated medially by the medial posterior projection of the meeting of the b2 and l2 cusp medial ridges in the intercuspal groove. The *aia* and *pia* of each tooth interlocks with the adjacent teeth in the postcanine row. The anterior of the tooth is m-shaped in occlusal view, formed by the convex anterior faces of b/l1. In the lower pcs the ridges of l/b1 embrace the base of cusps l/b2. Lower pcs have a single root, retaining the quadrate shape of the crown, and are straight-sided but indented bucco-lingually on the anterior face 1–2 mm ventrally to the base of the crown.

The maxilla is reduced and somewhat cylindrical in cross-section; it is more convex buccally and lingually, but flatter dorsally. There is a dorsal ridge running anteroposteriorly along the distal edge of the maxilla, and there are no lamina extending into the secondary palate or jugal.

Referred Specimens—MLR 20–22, MLR 20–38, G10174, TEMP2104, TEMP2105_4, TEMP2105_6, GLRCM G50137, GLRCM G50236, GLRCM G50505, GLRCM G50506, GLRCM G50507, GLRCM G50508, GLRCM G50647, GLRCM G50705, GLRCM G50907, GLRCM G51108, GLRCM G51221, GLRCM G51222, GLRCM G51223, GLRCM G51224, GLRCM G51243, GLRCM G51244, GLRCM G51245, GLRCM G51520, GLRCM G51521, GLRCM G51616, GLRCM G51823, GLRCM G51906, GLRCM G51907, GLRCM G52021, GLRCM G52022, GLRCM G52026, GLRCM G52027, GLRCM G52038, GLRCM G52127, GLRCM G52202, GLRCM G52204, GLRCM G52205, GLRCM G52304, GLRCM G52641, GLRCM G52643, GLRCM G52820, GLRCM G52861, GLRCM G53402, GLRCM G53403, GLRCM G53404, GLRCM G53405, GLRCM G53406, GLRCM G53407, GLRCM G53408, GLRCM G53409, GLRCM G53410, GLRCM G53411, GLRCM G53412, GLRCM G53413, GLRCM G53414, GLRCM G53415, GLRCM G53416, GLRCM G53417, GLRCM G53418, GLRCM G53419, GLRCM G53420, GLRCM G53421, GLRCM G53422, GLRCM G53423, GLRCM G53424, GLRCM G53425, GLRCM G53426, GLRCM G53427, GLRCM G53428, GLRCM G53429, GLRCM G53430, GLRCM G53431, GLRCM G53432, GLRCM G53433, GLRCM G53434, GLRCM G53435, GLRCM G53804, GLRCM G53806, GLRCM G53807, GLRCM G53809, GLRCM G53811, GLRCM G53812, GLRCM G54017, GLRCM G54018, GLRCM G54610, GLRCM G54633, GLRCM G54634, GLRCM G54635, GLRCM G54701,

GLRCM G54702, GLRCM G54703, GLRCM G54810, GLRCM G54811, GLRCM G55225, GLRCM G55226, GLRCM G55227, GLRCM G55534, GLRCM G55810, GLRCM G56416, GLRCM G56424, GLRCM G56425, GLRCM G56426, GLRCM G56433, GLRCM G510202, GLRCM G510203, GLRCM G510204, GLRCM G510205, GLRCM G510206, GLRCM G510207, GLRCM G510208, GLRCM G510209, GLRCM G510210, GLRCM G510211, GLRCM G75710: NHMUK PV M.36503, NHMUK PV M.36510, NHMUK PV M.36534, NHMUK PV M.36537; NHMUK R.8720, NHMUK PV M.36534, NHMUK PV M.36539, NHMUK PV M.36506, NHMUK PV M.36543, NHMUK PV M.46103, NHMUK PV M.46266, NHMUK PV M.46261, NHMUK PV M.45265, NHMUK PV M.46268, NHMUK PV M.46270, NHMUK PV M.46271, NHMUK PV M.46273, NHMUK PV M.46274, NHMUK PV M.46272, NHMUK PV M.46374, NHMUK PV M.46375, NHMUK PV M.46277, NHMUK PV M.46373, NHMUK PV M.46382, NHMUK PV M.46383, NHMUK PV M.46384, NHMUK PV M.46386, NHMUK PV M.46403, NHMUK PV M.46415, NHMUK PV M.46255 NHMUK PV M.46263, OUMNH J.21790, OUMNH J.79435, OUMNH J.79439, OUMNH J.79447, OUMNH J.79448, OUMNH J.79459, OUMNH J.79466, OUMNH J.79469, OUMNH J.79470, OUMNH J.79471, OUMNH J.79477, OUMNH J.79478, OUMNH J.79480, OUMNH J.79484, OUMNH J.79492, and OUMNH J.21790.

Synonymized Specimens—We consider the following specimens, all from the isle of Skye and some previously referred to *S. hebridicus*, to belong to *S. ooliticus*: BRSUG 20572, BRSUG 20573, BRSUG 20574, BRSUG 20575, BRSUG 29000–29002 and BRSUG 28996–28999; NMS G.1992.47.120 (comprising two

specimens in same matrix), NMS G.2017.17.1, NMS G.2017.17.2, NMS G.2017.17.3, NMS G.2017.17.4, NMS G.2017.17.5 and NMS G.2017.17.6.

DESCRIPTION

Holotype *S. ooliticus*

BGS GSM113834—The holotype of *S. ooliticus* is a fragment of left maxilla 20.3 mm long, between 3.15–3.48 mm deep dorsoventrally, and between 3.9–4.8 mm wide bucco-lingually, although some damage to the buccal side means the original width was slightly greater (Fig. 2). It was originally thought to be a dentary (Charlesworth 1854; Owen 1957), then re-identified as an right maxilla (Simpson, 1928) and then correctly identified as an left maxilla (Clark and Hopson 1985). The abrasion of the buccal maxilla surface has exposed portions of the postcanine roots. The lingual side is less damaged, and convex. The maxilla fragment sits in the original matrix, mechanically prepared out of the rock except for the dorsal surface. Digital reconstructions reveal the shallow depth of the maxilla dorsoventrally, and the lack of laminae extending upwards onto the facial part of the skull, laterally under the jugal, or medially to partially form the secondary bony palate (see Clark and Hopson, 1985:399) (Fig. 2). A ridge projects anteroposteriorly along the distal edge of the dorsal of the maxilla, but it is broken and missing below the posteriormost PCs.

There are three empty postcanine alveoli, followed by three postcanines, and then a final, posterior-most empty alveoli. This indicates at least seven teeth in the

tooth row. The postcanine cusp formula is 2-2-2. PCs are quadrate when viewed occlusally, with the medial cusp-row slightly offset posteriorly from the level of the lingual one, and the lingual cusp-row slightly further offset posteriorly from the medial one, making the crown rhomboidal. All the PCs are wider buccolingually than they are long anteroposteriorly. The cusps are arranged in three anteroposterior rows of two cusps each. All are broken and missing cusps. In each tooth (where cusps are intact) the anterior ridges of cusps L/M3, and B2 embrace the bases of cusps L/M2 and B1.

The anterior-most PC measures 5.7 mm from the tip of the broken M3 to the tip of the roots. The broken and incomplete crown of the PC measures 3.1 mm in length (anteroposteriorly) and what remains of the PC buccolingually is only 1.6 mm in width. It is the least complete PC in the row: only the midline cusps M2 and M3 remain, and both are heavily worn and broken (Fig. 3). The tip of the cusp of M2 is broken, revealing enamel and dentine layers. The tip and posterior slope of M3 is broken, the posterior slope is broken, with the missing portion of the posterior slope leaving a large gap between this and the subsequent tooth. The anterior of the PC is worn and broken, missing the M1 and *aia*. Only a small portion of the intercuspal grooves remain between M2/M3 and the missing buccal and lingual cusp rows. CT scans reveal that most of the roots of this PC are intact, although the crown is separated from the roots. The crown is also cracked between cusps M2 and M3.

The middle of the three PCs is the most complete, possessing all cusps except L3, and with complete roots. It measures 5.1 mm from the tip of M3 to the tip of the roots, and the crown is 3.4 mm in length (anteroposteriorly) and 3.6 mm in width (buccolingually). All of the cusps are worn and/or damaged, and all are missing

most of their enamel. This is the only tooth in which the vestigial cusp L1 is present and visible (Fig. 3). Vestigial cusps B0*,* M1 and L1 have been incorporated into the *aia,* but much of the *aia* is missing. There is a small cuspule posterior to, and displaced lingually from, the L2 cusp (Fig. 3E). The corresponding part of B1 cusp is missing. Comparison with the figure of this tooth by Owen (1857:fig. 5) indicates considerable damage since it was originally discovered and figured (discussed below).

The posterior-most PC measures 5.5 mm from the tip of the B1 (most complete cusp, but still broken at the tip) to the tip of the roots, and the crown is approximately 3.5 mm in length (anteroposterior) and 3.1 mm in width (buccolingual) - enough remains to estimate a pre-broken width of at least 3.5 mm. This PC is less complete than the middle PC: it is missing both lingual cusps, but retains the remaining cusps, although they are damaged. The tops of all cusps are broken, with B1 being the most intact, although missing enamel. The *aia* and *pia* are both worn, but vestigial cusps M1 and B0 remain visible, connected by the *aia* ridge.

The roots of the anterior and middle PCs in BGS GSM113834 comprise six branches, which are arranged in three anteroposterior rows of two branches each (Fig. 3). The buccal and lingual roots are larger, and thicker along their lengths, whereas the medial roots are thinner, shorter, and taper more steeply. In the posterior-most PC there are three roots in the medial row (Fig. 3F), giving a total of seven roots. In all PCs the four larger roots are more or less the same width for most of their length (although the posterior two are slightly wider than the anterior two) and taper at the tips. The pulp cavity is hollow in all of the roots.

The *aia* and *pia* on all three PCs in the holotype are badly worn, but some features remain visible. The *pia* projects posteriorly, with a ridge running bucco-lingually along the edge of the tooth. This fits into the *aia* of the next PC posteriorly in the toothrow, as seen between the middle and posterior-most PCs. The *aia* is also ridged bucco-lingually along the edge of the tooth, with vestigial cusps L1, M1 and B0 incorporated into the ridge. This is more clearly seen in the middle and posterior PCs in the CT scan (Fig. 3).

It is worth noting that the holotype of *S. ooliticus* is in a less complete state than when first discovered and later described by Owen (1857) (Fig. 3D). Over 150 years of handling has resulted in considerable damage to the postcanine teeth. Looking especially at the most complete, middle tooth in the row: the anterolingual edge is now missing and the L3 has also missing since Owen's original drawing was made. The M3 is missing the tip of the cusp and posterolingual edge, and the B3 is damaged bucally and posteriorly, with sections of the tooth missing entirely. The remaining portions of the tooth appear somewhat worn at the edges since Owen's drawing was made. This makes comparisons with new material somewhat problematic.

Holotype *S. hebridicus*

BRSUG 20572—The holotype for *Stereognathus hebridicus* is a large postcanine (Table 1) with the cusp formula 2-2-2 (arranged in three anteroposterior rows of two cusps) in a small fragment of jaw (Fig. 4). It was originally described as an upper left postcanine, but has since been identified as an upper right postcanine

(Clark and Hopson, 1985). It is 7 mm from the tip of the M2 to the tip of the roots, and the crown is approximately 5.1 mm in length (anteroposterior) and 5.4 mm in width (buccolingual). The morphology of this specimen agrees with that of *S. ooliticus*.

There is a small cuspule posterior to L2 and offset lingually (Fig. 4A). A root from the next tooth posteriorly in the tooth row remains intact in the fragment of jaw. It is positioned underneath the *pia*, midway between the two widely spaced posterior roots. There were originally six roots: the two posteriormost roots are still present, encased in a small amount of maxilla material (Fig. 4), but their tips are broken. The two larger anterior roots and the smaller antero-medial roots are broken where they meet the tooth base, but the hole for their pulp cavity is still visible.

Paratypes *S. hebridicus*

BRSUG 20573—This badly damaged upper right postcanine, originally referred to *S. hebridicus*, is missing much of the lingual cusps and M2, and the tips of the remaining cusps (Fig. 5A-E). The crown measures 4.8 mm in length (anteroposterior) and 5.4 mm in width (buccolingual). The morphology is congruent with the holotype of *S. ooliticus*. Vestigial cusps M1 and B0 are still visible, incorporated into what remains of the *aia* ridge. The *pia* projects strongly posteriorly, with distinct indentations and ridges along its length, and a pit in the midline to receive the M1 of the next PC in the tooth row. Cusp B1 lacks a posterior cuspule, while L2 is broken in the region one would be found, if present. The bases of only five of the roots remain, as the postero-medial part of the tooth is damaged (Fig. 5F).

BRSUG 20574—This specimen is a lower left pc originally referred to *S. hebridicus*, but with morphology consistent with the lower postcanines of *S. ooliticus*. The crown measures 5.1 mm in length (anteroposterior) and 3.2 mm in width (buccolingual). The buccal side of the pc, including cusps, is well preserved, but the lingual side is damaged with some enamel missing and both cusps broken (Fig. 6A-E). The anterior side of each cusp is convex. The lingual ridge extending from cusp b1 terminates at the base of b2 ventrally to the cusp apex. This feature cannot be compared to the lingual side due to damage.

The *aia* is a ridged bucco-lingual shelf, and projects ~1 mm anteriorly from the crown. This area is m-shaped in occlusal view. The posterior edge of the pc is almost straight, and is slanted due to the anteroposterior cusp rows being offset, giving the tooth a rhomboidal appearance. There is no cingulid, but the buccal edge of the tooth forms an anteroposterior ridge that we term a pseudo-cingulid (Fig. 6E). Beneath the crown the tooth pinches inwards before the single, quadrangular root extends straight ventrally. This root is broken, extending only 1–2 mm ventrally below the posterior half of the crown. Some fragments of root and matrix are embedded in the hollow of the tooth.

BRSUG 20575—This lower left pc is in poor condition, missing portions of enamel, all of the cusp tips, and the entire l2 cusp and portion of the tooth (Fig. 6F–J). It was originally referred to *S. hebridicus*, but has morphology congruent with the lower postcanines of *S. ooliticus*. The crown measures 5.8 mm in length (anteroposterior) and 3.8 mm in width (buccolingual). The *pia* is missing on the lingual side and damaged on the buccal side, but what remains retains a similar shape to that of paratype BRSUG 20574. BRSUG 20575 has a strong pseudo-

cingulid running anteroposteriorly on the buccal side of the pc. The quadrangular root is broken, extending only up to 2mm, and the pc is hollow inside. There is a bucco-lingual indent on the anterior face of the root, just less than 2 mm ventrally to the base of the crown.

New Material from Skye

NMS G.2017.17.2—This specimen is an upper left postcanine that we refer to *S. ooliticus*. NMS G.2017.17.2 is currently the most intact upper PC of *Stereognathus* to be described, retaining most of the enamel, almost wholly intact cusps, and intact *aia* and *pia* (Fig. 5G–M). The morphology is as for *S. ooliticus*: the crown has a cusp formula of 2-2-2; deep V-shaped intercuspal grooves; longitudinal cusp rows offset anteroposteriorly; the tooth is quadrangular in occlusal view; and it is wider than it is long. The crown measures 3.8 mm in length (anteroposterior) and in 4.3 mm width (buccolingual).

NMS G.2017.17.2 has indents along the *pia* and *aia* for interlocking with the preceding and succeeding PCs in the tooth row. The *aia* is almost unworn and exhibits multiple cuspules and crenulations along the ridge, and in the position of the vestigial cusps (Fig. 5G and M). NMS G.2017.17.2 also has distinct cuspules posterior to L2 and B1, displaced lingually and bucally, respectively.

NMS G.1992.47.120—This specimen is a lower right postcanine that we refer to *S. ooliticus*. NMS G.1992.47.120 is currently one of the most intact lower pcs of *Stereognathus* to be described, being almost completely intact apart from the root, retaining all cusps, and with enamel still present (Fig. 7). The crown measures 5.7 mm in length (anteroposterior) and 3.6 mm in width (buccolingual). As in *S. ooliticus:*

cusp formula 2-2; deep V-shaped intercuspal groove; tooth is quadrangular in shape in occlusal view; has equal sized cusps; it is longer than it is wide; and the ridges running from b1 and l1 embrace the bases of cusps b2 and l2. The anterior of each cusp is convex, the posterior of the pc is almost straight, slanting slightly because the longitudinal cusps are offset anteroposteriorly. The buccal side of the pc is straighter than the lingual side in occlusal view, and the buccal edge of the crown has a pseudocingulid, as in *S. ooliticus* lower pcs and *S. hebridicus* paratypes BRSUG 20574 and BRSUG 20575.

The *pia* on NMS G.1992.47.120 is deep and well defined, divided almost into two by the point where the medial ridges of the l2 and b2 meet in the intercuspal groove and project posteriorly. The embayments of the *pia* are pitted and ridged, containing vestigial cusps b3 and l3 (Fig. 7B and G). The *aia* is most clearly seen in Fig. 7E; the anterior edges of b1 and l1 are convex, creating an m-shaped appearance in occlusal view, and project anteriorly to create a shelf that provides the point of contact with the *pia* of the preceding tooth.

Measurements

The size of postcanine tooth specimens attributed to *S. ooliticus* and *S. hebridicus* falls along a range we interpret as ontogenetic variation (Table 1, Fig. 8–9). The lower postcanines for each species have a similar size distribution (Table 2), with most specimens between 5.1–5.5 mm in length, 3.1–4 mm in width.

The upper postcanines do not share the same distribution for each putative species, according to our samples. Those attributed to *S. ooliticus* have modes of

3.1–3.5 mm in length and 3.6–4.0 mm in width, and those to *S. hebridicus* have modes of 4.1–4.5 mm length and 5.1–5.5 mm width. The distribution of *S. hebridicus* upper PCs – unlike the lowers of either putative species or the uppers of *S. ooliticus* – are bimodal for both length and width. They have two peaks in distribution: in length 3.1–3.5 mm and 4.1–4.5 mm, and in width 2.6–3 mm and 5.1–5.5 mm.

The mean of the measurements is similar between both species, except for the width of the uppers, which is 3.8 mm in *S. ooliticus* and 4.6 mm in *S. hebridicus* (Table 2). The sample of *S. hebridicus* specimens was two to three larger than for *S.ooliticus*, (Table 2). The largest range in the sample was among *S. hebridicus* lower pc length, and the smallest range was in *S. ooliticus* lower width.

To test whether there was a difference in size between the two putative species, we carried out Mann-Whitney U tests on length, width and ratios (width/length) of upper and lower postcanines for *S. ooliticus* and *S. hebridicus*. The null hypothesis was that there was no difference in the median size of each species. We rejected the null hypothesis in only two instances: when comparing the width of the upper PCs, and comparing the ratio of the upper PCs (which depends, in part, on width) including incomplete specimens for which measurements were estimated. For all other measurements (lower pc width, length and ratio, and upper PC length), and when estimated lengths were removed from the dataset, there was no statistically significant difference between samples.

When estimated measurements are included *S. hebridicus* appears to have wider upper PCs than *S. ooliticus*. However, when excluding estimates there is no statistically significant difference between putative species: therefore we argue that

this statistical result is most likely artefactual, and stems from conservatively estimated measurements used to achieve larger sample sizes for analysis. There is no corresponding significant difference found in the length of the upper PCs when estimated measurements are included. When estimated measurements are included there is also no corresponding difference in the sizes of the lower pcs, with which the uppers must occlude.

We therefore conclude that the measurement differences in upper PC width and ratio of upper postcanine length/width between the English and Scottish teeth is an artefact of estimating measurements, and not evidence that they belong to two distinct species.

DISCUSSION

Synonymizing *S. ooliticus* and *S. hebridicus*

Recognition of the size and morphological variability within *Stereognathus* allows for a systematic reassessment of *S. hebridicus*. We find no clear diagnostic differences between *S. hebridicus* and *S. ooliticus*, either in size or morphology. We therefore synonymize *S. hebridicus* with *S. ooliticus*.

The original diagnosis for *S. hebridicus* stated that this second species was "1.6 times" larger in size than the type species, *S. ooliticus* (Waldman and Savage 1972). This size difference was determined on the basis of four isolated postcanines of *S. hebridicus* from Skye, of which only two were upper postcanines that could be

compared with the *S. ooliticus* holotype. No other characters distinguishing it from *S. ooliticus* were identified, as the authors awaited “full preparation of the material” from Skye before clarifying the diagnosis and anatomy of *S*. *hebridicus* (Waldman and Savage, 1972:122). However, the complete description and taxonomic assessment were never carried out. A comprehensive study of specimens assigned to *Stereognathus* more generally - both *S*. *hebridicus* and *S*. *ooliticus* - has not previously been undertaken.

Re-examination of all available *Stereognathus* postcanine material in the UK indicates that although the holotype PC of *S. hebridicus* is indeed larger than the holotype of *S. ooliticus*, when all *Stereognathus* postcanine tooth specimens are analysed together it appears that all material - including both English and Scottish specimens - comprise a spectrum of size with no discernible clustering between large and small morphs (Fig. 8). Results of the Mann-Whitney U test found no statistically significant differences in measurements, except upper PC width, and ratio of upper PC width/length when estimated measurements of incomplete postcanines were included (Table 2). There is no corresponding difference in the length, width or ratio of the lower pcs in the data including estimates, and no statistical difference at all when estimated measurements are not included. A correspondence between upper and lower postcanine size distribution would be expected, as uppers and lowers of drastically different sizes could not easily occlude with one another. We suggest that the evidence from the lower pcs and the length of the upper PCs of specimens attributed to each *Stereognathus* species indicates that size is not a diagnostic feature separating a purportedly larger species (*S. hebridicus*) from a smaller one (*S. ooliticus*). The spectrum of variation is probably

best explained by ontogenetic variation, coupled with drawbacks in estimating measurements.

The mechanism for tooth replacement in tritylodontids is a 'conveyor-belt' system in which teeth are added at the posterior end of the tooth row and lost at the anterior end at the diastema (Kühne, 1956; Matsuoka and Setoguchi, 2000). As a result, isolated tritylodontid postcanines are relatively abundant in the fossil record where tritylodontids occur in the UK (although mostly fragmentary). The advantage of this is the possibility of recovering postcanines from many ontogenetic stages, revealing information on the size range of these cyndodonts. Our measurements (Table 1, Fig. 8–9) reflect this range of ontogenetic size variation.

Although some tritylodontids are possibly sexually dimorphic (Kühne, 1956; Hopson and Kitching, 1972; Matsuoka et al., 2016), we do not see any clear clustering between possible male and female morphs in our data. However this may be due to sample size, and such clustering could possibly become apparent if a larger sample was available to us. At the very least, the size of our sample is adequate to show that there is no clear size distinction between the English and Scottish material. For that reason, coupled with the fact that there are no discrete character diagnostic differences among them, we refer them to the same single species, which is *S. ooliticus* by priority.

In terms of discrete characters, there is no strong evidence to support *S. hebridicus* as a distinct species from *S. ooliticus*, either in the upper or in the lower postcanine morphology. Assessing potential species level apomorphies in all known specimens has proven difficult due to the fragmentary nature of the fossils; many

features were missing due to damage or wear. This also meant comparisons of specific characters between fossil localities cannot easily be made. However, where features are present it appears there is some variability, but it is not of the variety in which English specimens have one condition and Scottish specimens another. Specimens previously assigned to the two different species share characters, whereas others assigned to the same species do not. Preservation and tooth wear plays a greater role in interpretation than often acknowledged. The often damaged and fragmentary nature of the fossil record for this genus is reflected in our data, because many features could not be observed even in these most complete specimens. And, our study has also revealed some new variable features. For example, the cuspules posterior to L2 and B2 in *Stereognathus* have not previously been identified, but are present in material from multiple localities.

Despite the lack of morphological evidence for there being two distinct species, we cannot definitively rule out that these geographically separated populations—the more northern Scottish vs. the more southern English faunas—had not undergone some degree of biological speciation that is not reflected in our tooth-based morphological comparisons. However this is not supported by the current fossil evidence. Future discoveries may shed further light on this.

To date, very little morphological description has been carried out for lower postcanines of *Stereognathus*, and no formal diagnostic characters have been identified (some features, such as the interlocking areas, were described but not used diagnostically, for example in Ensom, 1994). Here we have formally identified several morphological characters of the lower postcanines, which are present in both English and Scottish specimens: the projection of the *aia*; the *pia* comprising two

embayments, pitted inside; the *pia* framed by the termination of the b2 and l2 cusp ridges buccally and lingually, and separated medially by the posterior projection of the meeting of the b2 and l2 cusp medial ridges in the intercuspal groove; the m-shaped anterior of the pc in occlusal view; single root that retains the quadrate shape of the crown, and is indented bucco-lingually on the anterior face (Fig. 6–7). Whether the pseudo-cingulid, identified in more complete lower pc material, is a diagnostic morphological character, or whether it develops as a result of wear during occlusion, is uncertain given the incompleteness of *Stereognathus* material. Further investigation may reveal more about the pattern of occlusion in Tritylodontidae, particularly in more derived taxa.

Comparisons

All *Stereognathus* possess the sharp corners and quadrangular shape in both upper and lower postcanines as originally described in *S. ooliticus* (Owen, 1857). *Stereognathus* shares this feature with *Polistodon* (He and Cai, 1984), *Xenocretoschus* (Tatarinov and Mashenko, 1999) and *Montirictus* (Matsuoka et al., 2016). This is in contrast to the rounder shape of all other tritylodontid genera.

Upper and lower molar cusps in *Stereognathus* are of more or less equal in size (damage and wear permitting), which is also the case in *Xenocretosuchus, Polistodon* and *Montirictus*, but unlike in *Oligokyphus*, *Kayentatherium*, *Lufengia, Dinnebitodon, Yuanotherium*, *Bienotherium*, *Nuurtherium* or *Shartegodon*, in which cusp size is variable. A faint pseudo-cingulid visible on the buccal edge of the crown of the lower pcs has also been described for *Polistodon* (He and Cai, 1984).

Stereognathus and recently described genus *Montirictus* from Japan (Matsuoka et al., 2016) share a great number of similarities, suggesting a close relationship between these genera. *Montirictus* upper PCs also possess three rows of two cusps, and well-developed anterior and posterior interlocking areas. Matsuoka et al., (2016) described the vestigial cusps as absent in larger individuals and considered the vestigial M1 cusp to be a separate feature from the *aia* protrusions, located instead on the crescentic anterior cusp face of the M2. We consider the vestigial cusp M1 to be present in *Montirictus* and incorporated as part of the *aia* ridge, as in *Stereognathus*. The teeth of *Montirictus* are quadrangular in shape like in *Stereognathus*. Both genera have v-shaped intercuspal grooves that meet subequally (nearly equally), a character they share with *Xenocretosuchus* (Tatarinov and Mashenko, 1999; Lopatin and Agadjanian, 2008) and *Polistodon* (He and Cai, 1984), and which is often modified or removed by wear.

Stereognathus had at least seven upper postcanines in the tooth row. Tritylodontids possessed between five (*Yunannodon, Bocatherium*) and 13 (*Polistodon*) upper PCs (the functional tooth count in *Polistodon* was not reported and is now difficult to determine as the holotype is glued in occlusion, with bones of the dentary and jugal obscuring the rear of the tooth row). The posteriormost PC was not yet, if ever, fully erupted (He and Cai, 1984). Non-functional posterior-most PCs, and heavily worn and presumably soon-to-be-lost anterior-most PCs, are present in various specimens due to the ‘conveyor belt’ mode of dentition in which teeth move anteriorly, with the oldest teeth falling out at the diastema, and new replacement teeth being added at the back of the tooth row. This makes exact tooth count an unreliable character to compare among tritylodontids, as differences observed in

specimens could be the result of capturing different moments in the tooth replacement process, rather than a diagnostic difference in tooth count between two individuals or species. Tooth count can also be variable between different sides of the same animal (Clark and Hopson 1985; Young, 1982; He and Cai, 1984; Matsuoka and Setoguchi 2000; Watabe et al., 2007), the same is true for lowers. If there is a close relationship between *Stereognathus* and *Polistodon* (Watabe et al., 2007), suggests the potential for a higher tooth count in the upper tooth row of *Stereognathus,* as recorded for *Polistodon* (He and Cai, 1984). More material is needed to address this.

The upper PCs of *Stereognathus* have a cusp formula of 2-2-2. This differs from *Tritylodon* (Owen 1884), *Oligokyphus* (Hennig 1922), *Bienotherium* (Young, 1940), *Lufengia* (Chow and Hu, 1959), *Yunnanodon* (Cui, 1976), *Dianzhongia* (Cui, 1981), *Bienotheroides* (Young 1982), *Kayentatherium* (Kermack 1982; Sues, 1986), *Dinnebitodon* (Sues, 1986), *Yuanotherium* (Hu. Meng and Clark, 2009), *Shartegodon* and *Nuurtherium* (Velazco et al., 2017), which all have a higher number of cusps in one or more rows.

The ratio of width/length has been used diagnostically by other authors; we found the lower postcanines of *Stereognathus* varied from 0.60–0.86, and uppers between 0.79–1.41 (Table 1). These measurements for tritylodontids are vulnerable to error as many specimens are missing enamel and have varied degrees of tooth wear. However it remains useful between genera.

Previous authors have identified only five roots in *Stereognathus*, and this has then been repeated by subsequent authors, particularly in character analysis. We

show here based on CT data that this root count is incorrect. This indicates that it may be necessary to CT scan and recount the root numbers in some other tritylodontid specimens. The roots of *Stereognathus* upper PCs instead vary in number between six and seven, potentially connected with their position in the tooth row (with more roots in posterior PCs). *Montirictus* also has six roots, but the roots of *Montirictus* compress inwards more tightly below the crown, and orient outwards again ventrally. According to Cui and Sun (1987) *Bienotherium*, *Lufengia*, *Yunnanodon* and *Bienotheroides* all have five roots, *Nuurtherium* also has five roots, and *Shartegodon* has four (Velazco et al., 2017). Cui and Sun (1987) observed that *Lufengia* has some fusion or dental laminae between the roots as in *Oligokyphus* (Kühne, 1956). However, various authors have identified only five roots in *Stereognathus*, and this has then been repeated by subsequent authors, particularly in character analysis. We show here that this root count is incorrect, based on our CT data. This indicates that it may be necessary to CT scan and recount the root numbers in some other tritylodontid specimens. *Oligokyphus* is described as having five roots connected transversely in two rows by dental laminae (Kühne, 1956). Such laminae are mostly absent in *Stereognathus*, although the medial roots are sometimes joined anteroposteriorly into a row (see posteriormost PC in BGS GSM113834, Fig. 3F). The extent of this joining appears to be variable.

In BRSUG20572, there is a large root in situ between the posterior roots of the PC, which by morphology and position belongs to the next tooth in the tooth row (absent) (Fig. 4). However, the medial placement of this larger PC root does not follow the morphology of medial roots in the tooth row seen in the holotype BGS GSM113834. Because complete and well-preserved material is so rare, this unusual

placement may have been more widespread in *Stereognathus*, it may be a post-depositional artefact, or the result of the conveyor belt movement of the PCs along the room row. This conveyor belt movement has been observed in other specimens of Tritylodontidae to produce an increasing curvature of the roots underneath the preceding postcanine, notably in the lower pcs (Cui and Sun 1987; Matsuoka et al., 2000).

The lower pcs of *Stereognathus* have a cusp formula of 2-2, which differs from *Oligokyphus* (Kühne, 1956) and possibly *Tritylodon* (Fourie, 1963) which have the formula 3-3. The 2-2-2/2-2 PC/pc cusp formula is shared with, *Polistodon* (He and Cai, 1984), *Bocatherium* (Clark and Hopson, 1985), *Xenocretosuchus* (Tatarinov and Matschenko, 1999), *Montirictus* (Matsuoka et al., 2016), *Shartegodon* and *Nuurtherium* (Velazco et al., 2017). Although *Bienotherium* and *Kayentatherium* share the 2-2 cusp formula in the lower pcs, the anterior cusps of both genera are larger than the posterior cusps (Young, 1947; Kermack, 1982), whereas in *Stereognathus, Xenocretosuchus, Montirictus, Shartegodon* and *Nuurtherium* the cusps are equal. The lower postcanines of *Stereognathus* most closely resemble those of *Xenocretosuchus* and *Montirictus* in morphology, and also bear close resemblance to the recently described *Shartegodon* and *Nuurtherium* (Velazco et al., 2017). They are all quadrangular and rhomboidal in appearance, and *Stereognathus,* and *Xenocretosuchus* possess vestigial (l3) and (b3) cuspules within the *aia* and *pia* (Tatarinov and Mashenko, 1999). The interlocking areas in *Stereognathus* are especially similar to those described in *Xenocretosuchus kolossovi* (Lopatin and Agadjanian, 2008), as the two taxa share the same ridges of chaotic enamel inside the embayments where the next tooth in the row ‘locks’ into place. This is also

described for *Montirictus* (Matsuoka et al., 2016). These vestigial cusps are not mentioned in *Shartegodon* or *Nuurtherium*; however we suggest they may be present in *Shartegodon* (Velazco et al., 2017:fig. 9).

The roots of the lower postcanines of *Stereognathus* show a similar morphology to those of *Xenocretosuchus, Montirictus, Shartegodon* and *Nuurtherium* in being box-like and extending straight downwards from the crown. Although in *Stereognathus* the ventral-most section of a pc has not yet been recovered, the specimens we examined shared the concave ridge 2–3 mm ventrally below the *aia* as present in *Montirictus* (Matsuoka et al., 2016:fig. B3–4, C3). This feature is pronounced in *Montirictus*: the anterior face of the root is directed posteroventrally at an angle into this concavity, before bulging anteriorly below the concavity. The root also bifurcates below the line of concavity, with the anterior-most root-half curving posteriorly at the ventral tip (Matsuoka et al., 2016). In *Shartegodon* (and possibly *Nuurtherium*) the root also curves as in *Montirictus*, but there is no bifurcation in the ventral part of the tooth, and the ridge identified for *Stereognathus* and *Montirictus* is not evident (Velazco et al., 2017:fig. 10). This s-shape (referred to as ‘c-shaped” in Velazco et al., 2017) curving is similar to that seen in other tritylodontid pcs, but more pronounced and angular in appearance in *Montirictus* and *Shartegodon,* echoing the shape of the tooth crown. The lower pcs DORCM-G10828 from the Forest Marble, and GLRCM TEMP6036 from Hornsleasow, retain the most complete pc *Stereognathus* roots. They follow a *Montiricus/Shartegodon*-like pattern (Panciroli, pers. obs.), but are not complete and therefore we cannot confirm the ventralmost morphology of the root. The same is true for as yet undescribed material recently

recovered from Woodeaton (Panciroli, pers. obs.). More complete lower postcanine material is required.

Stereognathus lower pcs resemble *Xenocretosuchus* (Lopatin and Agadjanian, 2008), *Montiricutus* (Matsuoka et al., 2016), *Shartegodon* and *Nuurtherium* (Velazco et al., 2017) in having the buccal cusp row slightly posteriorly offset from the lingual row, and in the morphology of the *pia*: forming two embayments separated by the l2/b2 medial ridges meeting in the intercuspal groove and projecting posteriorly. In *Xenocretosuchus*, the ridges extending from the cusps into the intercuspal grooves were described as connecting in one intercuspal groove, but not the other (Lopatin and Agadjanian, 2008). However, this intercuspal groove is often modified by wear, and therefore this is not reliably diagnostic in either genus.

Phylogenetic Analysis

Many previous character analyses of Tritylodontidae place *Stereognathus* in a clade that includes *Bocatherium, Polistodon*, *Xenocretosuchus* and *Montirictus* (Watabe et al., 2007). Most studies agree that *Oligokyphus* is the most basal member of Tritylodontidae, and consider *Stereognathus, Bocatherium*, *Bientheroides, Xenocretosuchus* and *Montirictus*, to be “advanced” tritylodontids (Clark and Hopson, 1985; Sues, 1986; Setoguchi et al., 1999; Watabe et al., 2007). However only dental remains and two incomplete maxillae have been found and described for *Stereognathus*.

Clark and Hopson (1985) placed *Stereognathus* in a clade with *Bocatherium* and *Bienotheroides* based on the absence of facial, palatine and zygomatic

processes. Some characters were applied to *Stereognathus* “by inference” (p399), based on resemblances between the holotype of *S. ooliticus* and more complete material for *Bocatherium* and *Bienotheroides*. They describe a “prominent groove on the maxilla” of *S. ooliticus* as an indication that it possessed an infraorbital foramen at the junction of the premaxilla, jugal and lacrimal. This groove is not clear either by direct observation or in CT-scan reconstruction, and so we cannot confirm that *Stereognathus* possessed this character. *Stereognathus, Bocatherium* and *Bienotheroides*, *Dinnebitodon*, and *Yuanotherium* all share a uniquely reduced and cylindrical maxilla (referring to the convexity of the buccal and lingual sides, although cross-sectionally the maxilla of *Stereognathus* is somewhat rectangular), lacking laminal extensions into the face (Clark and Hopson, 1985:399). This highly derived character, along with the reduction to only two principle cusps per longitudinal row in the upper postcanines, supports grouping these tritylodontids into a clade.

The cladistic analysis by Watabe et al. (2007) used 17 taxa and 11 characters, six of which are dental. Watabe et al. scored the vestigial cusps as absent in *Stereognathus*, which we see from our reassessment is not the case. They also scored five cranial characters based on Clark and Hopson (1985), most of which were inferred (see above discussion). Their data were compiled second hand from multiple sources, concluding that these data were not sufficient at that time to satisfactorily resolve the polytomies among Tritylodontidae; namely between *Stereognathus, Montirictus, Polistodon, Xenocretosuchus*, and *Bocatherium,* and between *Kayentatherium, Lufengia,* and *Diangzongia*. They suggested that additional characters are required to do so.

The most recent character analysis was carried out by Velazco et al. (2017), using 35 characters (22 skeletal and 13 dental). *Stereognathus* was scored on 15 of these characters: nine dental and six skeletal. The tree presented in their paper (Velazco et al., 2017:fig 16), was not the strict consensus tree of four most parsimonious trees of 68 steps as stated (elsewhere it is stated that there were two parsimonious trees (Velazco et al., 2017:28), but there were four). Unfortunately there is also an error in their character matrix in the appendix for their paper. We obtained the correct matrix from Morphobank, and re-ran the tree analysis using their methods to obtain their strict consensus tree. This places all tritylodontids in an unresolved polytomy, with the exception of *Oligokyphus* (outgroup) and *Tritylodon* as most basal, and a separate clade containing *Nuurtherium*, *Shartegodon* and *Yuanotherium* in an unresolved polytomy.

Our re-analysis of *Stereognathus* clarifies certain characters, such as root count, and finds no support for other characters, such as a post incisive snout constriction. We re-ran the Velazco et al. (2017) analysis with *Stereognathus* rescored (Appendix 1–2). Five of the six skeletal characters we rescored as unknown (characters 1, 2, 7, 8, 14). These characters were previously scored based on Clark and Hopson (1985), as mentioned previously, regarding inferences about the facial, palatine and zygomatic processes for which we find no support. We retained the reduction of the maxilla as highly reduced (character 12), and the absence of a lateral extension of the maxilla (character 16), and added absence of the palatine contributing to the PC4 alveolus (character 14). The dental characters we retained were the cusp formula of upper PCs as 2-2-2, the absence of M0 and L0, the large L3 cusp, and uncertainty over whether the lower postcanine bifurcates

or is single rooted (character 24, 26, 27, 30 and 34). We rescored characters 25, 28, 29, 31, 32, 33 and 35. These are (respectively) the presence of the B0 cusp, the presence of a small M1 cusp and small L1 cusp, six or seven roots in the upper PCs, the presence of an anterior median root, the generalised lower cusp formula of 2-2, and the long single root in the lower pc with a curve in the ventral-most portion (s-shaped).

Following Velazco et al. with updated characters for *Stereognathus* yields five parsimonious trees of 71 steps, and a strict consensus tree that is almost identical to the original, but with the polytomy between *Nuurtherium*, *Shartegodon* and *Yuanotherium* resolved, finding *Shartegodon* and *Yuanotherium* more closely related to one another than to *Nuurtherium* (Fig. 10A). In this matrix, six taxa have > 50% missing data, and three > 60% (*Yunannodon* 62.9%, *Montirictus* 65.7% and *Xenocretosuchus* 77.2%). *Stereognathus* has 60% missing data. Removing *Montirictus* and *Xenocretosuchus* yields three parsimonious tree of 70 steps, and results in a strict consensus tree identical to that found by Velazco et al., but with the addition of a clade formed by *Polistodon* and *Bocatherium*. *Stereognathus* remains part of the polytomy with most other tritylodontids.

Eliminating taxa with the most missing entries can alter the relationships among taxa, without clarifying them (Wilkinson, 2003). In order to avoid this, we ran an agreement subtree on the whole dataset with *Stereognathus* rescored, to identify the largest subset of taxa in all of the parsimonious trees that are identically related (Goloboff et al., 2008). This resulted in a tree with ten taxa, including *Stereognathus*, placing it as the nearest outgroup to *Shartegodon*, *Nuurtherium* and *Yuanotherium*

(Fig. 10B). Other than the addition of new taxa, this tree topology differs little from Clark and Hopson's (1985), despite including more characters and taxa.

In light of the difficulties coding only one of these tritylodontid taxa – *Stereognathus* - based on the previous literature, we consider phylogenetic analyses of tritylodontids will remain problematic and cannot be further resolved until comprehensive re-descriptions (to confirm or re-describe characters as necessary) of existing material are available. We also suggest that there may be more intraspecies variation in cusp shape and morphology than previously recognized - often confounded by poor preservation and degree of tooth wear - and that this variation may have occasionally been erroneously interpreted as apomorphic. We therefore consider phylogenetic analysis to be preliminary until more detailed, up to date information is available for the many poorly described or figured taxa, and particularly for taxa that were unresolved in our analysis, such as *Polistodon*, *Lufengia*, *Beinotheroides*, *Diangzhongia,* and *Bocatherium*. As is often the case, more complete material for other taxa, including *Stereognathus*, *Xenocretosuchus*, and *Montirictus* would almost certainly improve the resolution of future phylogenetic analysis.

CONCLUSIONS

Re-evaluating the UK collections of *Stereognathus*, we provide strong evidence to suggest that *S. hebridicus* is a junior synonym of *S. ooliticus*. The former was based on size, without a comprehensive description of morphology. Our

analysis indicates that the holotype, paratypes, and subsequently discovered *S. hebridicus* material falls along an ontogenetic size spectrum, overlapping the size range of *S. ooliticus*. There is no statistically significant difference in size distribution between postcanines attributed to these two putative species.

Morphological analysis finds many characters within *Stereognathus* are variable within the genus, as well as appearing variable due to cusp wear through occlusion and post-mortem damage. Despite this, we outline several important features of *Stereognathus*, including: cusp formula 2-2-2/2-2 PC/pc; subequal cusps with medial ridges of the cusps meeting in the intercuspal-groove subequally; cuspules posterior and distally to cusps L2 and B1 in upper PCs; vestigial cusps incorporated into the *aia* and *pia;* a bucco-lingual indent on the anterior face of the lower pc root, 1–2 mm ventrally to the base of the crown; and the maxilla reduced and somewhat cylindrical in cross-section with no lamina extending into the secondary bony palate or jugal.

Despite the need for considerable further studies redescribing existing species and identifying additional characters for phylogenetic analysis, the Tritylodontidae remain one of the most successful and long-lived cynodont groups, far outlasting other non-mammaliamorph cynodonts by persisting into the Early Cretaceous.

Although it is tempting to draw conclusions from the fragmentary remains for many tritylodontids, including *Stereognathus*, it is important to recognize the limitations of the current fossil evidence. Cusp wear can alter tritylodontid postcanines and lead to the erection of genera and species that may not stand the

test of time and confuse later research. For tritylodontids, it may be better to err on the side of caution, and focus on comprehensive re-evaluations of what, in many cases, are still poorly described collections. Upon these sturdier foundations new examinations of this fascinating, yet understudied, group can be built.

ACKNOWLEDGMENTS

This research would not have been possible without the NERC DTP studentship and the Palaeontographical Association's Richard Owen Research Fund, both awarded to EP. SLB is supported by Marie Curie Career Integration Grant EC630652, Royal Society Research Grant RG130018, and the University of Edinburgh. We would like to thank: I. Butler at the University of Edinburgh and T. Davies at the University of Bristol for their time and expertise acquiring CT scan data for this project; P. Brewer at the Natural History Museum in London, H. Ketchum from the Natural History Museum in Oxford, and D. Rice from Gloucester Museum for collections access; and R. Benson who ensured we had the most recent collected specimens from the Isle of Skye for scanning and comparison. Thank you to A. Averianov for sharing his group's work on Siberian tritylodontids, and to P. Velazco for his correspondence regarding the character matrix for phylogenetic analysis.

LITERATURE CITED

Charlesworth, E. 1854. Notice on new vertebrate fossils. Report of the British Association for the Advancement of Science 80.

Chow, M., and C. Hu. 1959. A new tritylodontid from Lufeng, Yunnan. Vertebrata PalAsiatica 3:7–10.

Clark, J. M., and J. A. Hopson. 1985. Distinctive mammal-like reptile from Mexico and its bearing on the phylogeny of the Tritylodontidae. Nature 315:398–400.

Cope, E.D. 1884. The Tertiary Marsupialia. American Naturalist 18:686–697.

Cui, G. 1976. Yunnania, a new tritylodont genus from Lufeng, Yunnan. Vertebrata PalAsiatica 3:85–90.

Cui, G. 1981. A new genus of Tritylodontoidea. Vertebrata PalAsiatica 19: 5–10.

Ensom, P. C. 1977. A therapsid tooth from the Forest Marble (Middle Jurassic) of Dorset. Proceedings of the Geologists' Association 88:201–205.

Ensom, P. C.1994. A lower postcanine of *Stereognathus*. sp. (Reptilia, Therapsida) from the Bathonian of Southern England. Proceedings of the Dorset Natural History and Archaeological Society 115:139–141.

Fedak, T. J., H.-D. Sues, and P. E. Olsen. 2015. First record of the tritylodontid cynodont *Oligokyphus* and cynodont postcranial bones from the McCoy Brook Formation of Nova Scotia, Canada. Canadian Journal of Earth Sciences 52:244–249.

Fourie, S. 1963. A new tritylodontid from the Cave Sandstone of South Africa. Nature 4876:201.

Goloboff, P. A., J. S. Farris, and K. C. Nixon. 2008. TNT, a free programme for phylogenetic analysis. Cladistics 24: 744–786.

He, X., and K. Cai. 1984. The tritylodont remains from Dashanpu, Zigong. Journal of Chengdu College of Geology (Special Paper on Dinosaurian Remains of Dashanpu, Zigong, Sichuan [II]):33–45.

Hennig, E. 1922. Die Säugerzähne der württembergischen Rhät-Lias-Bonebeds. Neues Jahrbuch für Mineralogie, Geologie und Paläontologie Beilage-Band 46:181–267

Holloway, S. 1983. The shell-detrital calcirudites of the Forest Marble Formation (Bathonian) of South West England. Proceedings of the Geologists' Association 94:259–266.

Hopson, J. A., and J. W. Kitching. 1972. A revised classification of cynodonts (Reptilia; Therapsida). Palaeontologica Africana 14:71–85.

Hu, Y., J. Meng, and J. M. Clark. 2009. A new tritylodontid from the Upper Jurassic of Xinjiang, China. Acta Palaeontologica Polonica 54:385–391.

Kemp, T. S. 2005. The Origin and Evolution of Mammals.Oxford University Press, Oxford, 344 pp.

Kermack, D. M. 1982. A new tritylodontid from the Kayenta formation of Arizona. Zoological Journal of the Linnean Society 76:1–17.

Kühne, W G. 1956. The Liassic therapsid *Oligokyphus*. British Museum (Natural History), London, 149 pp.

Lewis, G.E. 1986. *Nearctylodon broomi*, the first Nearctic tritylodont; pp. 295–303 in N. Hotton, P. D. Maclean, J. J. Roth, and E. C. Roth (eds.), The Ecology and Biology of Mammal-like Reptiles. Smithsonian Institution Press, Washington, DC.

Lopatin, A. V., and A. K. Agadjanian. 2008. A tritylodont (Tritylodontidae, Synapsida) from the Mesozoic of Yakutia. Dokaldy Biological Sciences 419:107–110.

Luo, Z.-X, Z. Kielan-Jaworowska, and R. L. Cifelli. 2002. In quest for a phylogeny of Mesozoic Mammals. Acta Palaeontologica Polonica 47:1–78.

Luo, Z.-X., and A. Sun. 1994. *Oligokyphus* (Cynodontia: Tritylodontidae) from the Lower Lufeng Formation (Lower Jurassic) of Yunnan, China. Journal of Vertebrate Paleontology 13:477–482.

Maisch, M. W., A. T. Matzke, and G. Sun. 2004. A new tritylodontid from the Upper Jurassic Shishugou Formation of the Junggar Basin (Xingjiang, NW China). Journal of Vertebrate Paleontology 24:649–656.

Matsuoka, H., and T. Setoguchi. 2000. Significance of Chinese tritylodonts (Synapsida, Cynodontia) for the systematic study of Japanese materials from the Lower Cretaceous Kuwajima Formation, Tetori Group of Shiramine Ishikawa, Japan. Asian Paleoprimatology 1:161–176.

Matsuoka, H., N. Kusuhashi, and I. J. Corfe. 2016. A new Early Cretaceous tritylodontid (Synapsida, Cynodontia, Mammaliamorpha) from the Kuwajima Formation (Tetori Group) of Central Japan. Journal of Vertebrate Paleontology. 36.4: e1112289.

Metcalf, S. J., R. F. Vaughan, M. J. Benton, J. Cole, M. J. Simms and D. L. Dartnall. 1992. A new Bathonian (Middle Jurassic) microvertebrate site, within the Chipping Norton Limestone Formation at Hornsleasow Quarry, Gloucestershire. Proceedings of the Geologists' Association 103:321–342.

Osborn, H. F 1903. The reptilian subclasses Diapsida and Synapsida and the early history of the Diaptosauria. Memoirs of the Armerican Museum of Natural History 1:449–507

Owen, R. 1857. On the affinity of *Stereognathus ooliticus* (Charlesworth) a mammal from the Oolitic slate of Stonesfield . Quarterly Journal of the Geological Society of London 13:1–11.

Owen, R. 1884. On the skull and dentition of a Triassic mammal (*Tritylodon longaevus*) from South Africa. Quarterly Journal of the Geological Society of London 40:146–152.

Parraga, J., E. Bernard, P. Brewer, D. J. Ward. 2016. A diverse new late Bathonian microvertebrate microvertebrate assemblage from Woodeaton Quarry, Oxfordshire, UK. Journal of Vertebrate Palaeontology Programme and Abstracts 2016: 202.

Rowe, T. B. 1993. Phylogenetic systematics and the early history of mammals; pp. 129–145 in F. S. Szalay, M. J. Novacek, and M. C. McKenna (eds.), Mammal Phylogeny: Mesozoic Differentiation, Multituberculates, Monotremes, Early Therians, and Marsupials. Springer-Verlag, New York.

Ruta, M., S. Botha-Brink, A. Mitchell, and M. J. Benton. 2013. The radiation of cynodonts and the ground plan of mammalian morphological diversity. Proceedings of the Royal Society B 280:20131865.

Setoguchi, T., M. Matsuda, and H. Matsuoka. 1999. New discovery of an Early Cretaceous trityldontid (Reptilia, Therapsida) from Japan and the phylogenetic reconstruction of Tritylodontidae based on the dental characters; pp. 117–124 in Y. Q. Wang and T. Deng (eds.), Proceedings of the Seventh Annual Meeting of the Chinese Society for Vertebrate Paleontology China Ocean Press, Beijing.

Simpson, G. G. 1928. A Catalogue of the Mesozoic Mammalia in the Geological Department of the British Museum. British Museum (Natural History), London.

Sues, H.-D 1985. First record of the tritylodontid *Oligokyphus* (Synapsida) from the Jurassic of Western North America. Journal of Vertebrate Palaeontology 5:328–335.

Sues, H.-D 1986. *Dinnebitodon amarali*, a new tritylodontid (Synapsida) from the Lower Jurassic of Western North America. Journal of Paleontology 60:758–762.

Sues, H.-D., and F. A. Jenkins Jr. 2006. The postcranial skeleton of *Kayentatherium wellesi* from the Lower Jurassic Kayenta Formation of Arizona and the phylogenetic significance of postcranial features in tritylodontid cynodonts; pp. 114–152 in M. T. Carrano (ed.), Amniote Paleobiology: Perspectives on the Evolution of Mammals, Birds, and Reptiles. The University of Chicago Press, Chicago.

Tatarinov, L. P., and E. N. Mashenko. 1999. A find of an aberrant tritylodont (Reptilia, Cynodontia) in the Lower Cretaceous of the Kemerovo Region. Palaontologicheskii Zhurnal 33:422–428.

Velazco, P. M., A. J. Buczek, and M. J. Novacek. 2017 Two new tritylodontids (Synapsida, Cynodontia, Mammaliamorpha) from the Upper Jurassic, southwestern Mongolia. American Museum Novitates 3874, 35 pp.

Waldman, M. and R. J. G. Savage. 1972. The first Jurassic mammal from Scotland. Journal of the Geological Society of London 128:119–125.

Watabe, M., T. Tsubamoto, and K. Tsogtbaatar. 2007. A new tritylodontid synapsid from Mongolia. Acta Palaeontologica Polonica 52:263–274.

Wilkinson, M. 2003. Missing entries and multiple trees: instability, relationships, and support in parsimony analysis. Journal of Vertebrate Palaeontology. 23:311–323.

Young, C-C. 1940. Preliminary notes on the Mesozoic mammals of Lufeng, Yunnan, China. Bulletin of the Geological Society of China 20:93–111.

Young, C-C. 1947. Mammal-like reptiles from Lufeng, Yunnan, China. Proceedings of the Zoological Society of London 117:537–597.

Young, C-C. 1982. On a *Bienotherium*-like tritylodont from Szechuan, China [in Chinese]; pp10–13 in Z. Yang (ed.), Selected works of Yang Zhongjian [in Chinese]. Science Press, Beijing.

FIGURE 1: Postcanine cusp terminology for *Stereognathus* used in this paper (modified from Watabe et al., 2007). The *pia* (posterior interlocking area) and *aia* (anterior interlocking area) are present on both teeth, but the *pia* is not visible in occlusal view on upper postcanines, and the *aia* is not visible in occlusal view on lower postcanines, because they are located on the underside of the tooth. [Intended for column width]

FIGURE 2: *Stereognathus ooliticus* holotype BGS GSM113834. **A_1** occlusal view; **A_2** occlusal view of CT-scan reconstruction, with teeth segmented from jaw; **B_1** buccal view; **B_2** buccal view of CT-scan reconstruction, with teeth segmented from jaw; **C_1** lingual view; **C_2** lingual view of CT-scan reconstruction, with teeth segmented from jaw; **D** dorsal view of maxilla. Anterior direction indicated by longer black arrow, lingual by shorter arrow. [Intended for whole page width]

FIGURE 3: *Stereognathus ooliticus* holotype BGS GSM113834, postcanines only. Digitally reconstructed from microCT-scans and segmented from the jaw. **A** occlusal photograph of anteriormost PC; **B** occlusal photograph of middle PC; **C** occlusal photograph of posteriormost PC; **D** original drawing by Owen (1856); **E** occlusal view of digitally reconstructed tooth row: **F** dorsal view of digitally reconstructed tooth row; **G** anterolingual view of digitally reconstructed tooth row; **H_1** anterior view of anteriormost PC; **H_2** posterior view of anteriormost PC; **I_1** anterior view of middle PC; **I_2** posterior view of middle PC; **J_1** anterior view of posteriormost PC; **J_2** posterior view of posteriormost PC. Anterior direction indicated by longer black arrow, lingual by shorter arrow. [Intended for whole page width]

FIGURE 4: Holotype of *Stereognathus hebridicus* BRSUG 20572. **A_1** photograph of occlusal surface; **A_2** occlusal view from digital reconstruction of CT-scan; B dorsal view; **C_1** photograph of anterior view; **C_2** digital reconstruction of anterior view; **D** buccal view; **E_1** photograph of posterior view; **E_2** digital reconstruction of posterior view; **F** lingual view. Anterior direction indicated by longer black arrow, lingual by shorter arrow. [Intended for 2/3 page width]

FIGURE 5: Paratype of *Stereognathus hebridicus* upper postcanines BRSUG 20573, and new specimen NMS G.2017.17.2, both reconstructed digitally from CT-scans. **A-F** BRSUG 20573: **A_1** occlusal surface; **A_2** occlusal surface digital reconstruction; **B_1** anterior view; **B_2** anterior view digital reconstruction; **C_1** posterior view; **C_2** posterior view digital reconstruction; **D_1** lingual view; **D_2** lingual view digital reconstruction; **E_1** buccal view; **E_2** buccal view digital reconstruction; **F** dorsal view. **G-M** NMS G.2017.17.2: **G_1** occlusal surface; **G_2** occlusal surface digital reconstruction; **H_1** anterior view; **H_2** anterior view digital reconstruction; **I** posterior view digital reconstruction; **J** lingual view digital reconstruction; **K** buccal view digital reconstruction; **L** dorsal view; **M** ventrolingual view. Anterior direction indicated by longer black arrow, lingual by shorter arrow. [Intended for whole page width]

FIGURE 6: Paratypes of *Stereognathus hebridicus* lower postcanines BRSUG 20574 and BRSUG 20575. **A-E** BRSUG 20574: **A_1** occlusal view; **A_2** occlusal surface digital reconstruction; **B_1** posterior view; **B_2** posterior view digital reconstruction; **C_1** anterior view; **C_2** anterior view digital reconstruction; **D_1** lingual view; **D_2** lingual view digital reconstruction; **E_1** buccal view; **E_2** buccal view digital reconstruction. **F-J** BRSUG 20575: **F_1** occlusal view; **F_2** occlusal surface digital reconstruction; **G_1** posterior view; **G_2** posterior view digital reconstruction; **H_1** anterior view; **H_2** anterior view digital

reconstruction; **I_1** lingual view; **I_2** lingual view digital reconstruction; **J_1** buccal view; **J_2** buccal view digital reconstruction. Anterior direction indicated by longer black arrow, lingual by shorter arrow. [Intended for whole page width]

FIGURE 7: New specimen NMS G.1992.47.120, a lower postcanine reconstructed digitally from CT-scans. **A_1** occlusal surface; **A_2** occlusal surface digital reconstruction; **B** posterior view reconstruction; **C** anterior view digital reconstruction; **D_1** lingual view; **D_2** lingual view digital reconstruction; **E** anterolingual view; **F_1** buccal view; **F_2** buccal view digital reconstruction; **G** posterobuccal view. Anterior direction indicated by longer black arrow, lingual by shorter arrow. [Intended for whole page width]

FIGURE 8: Scatterplots of postcanine measurements of *Stereognathus*. **A** shows upper postcanines, **B** shows lower postcanines. Key for **B**, as in **A**. Complete specimens are filled shapes (orange square = *S. ooliticus*, blue diamond = *S. hebridicus*) incomplete are not filled. Measurements in Table 1. [Intended for column width]

FIGURE 9: Distribution of *Stereognathus* postcanine specimens. **A** is upper PC length, **B** is upper PC width, **C** is lower pc length, **D** is lower pc width. Orange striped = *S. ooliticus*, blue non-striped = *S. hebridicus*. [Intended for 2/3 page width]

FIGURE 10: Trees generated by our phylogenetic analysis of tritylodontid taxa, using updated characters for *Stereognathus*. **A** is the strict consensus of the five parsimonious trees of 71 steps. **B** is the agreement subtree of 10 taxa. [Intended for 2/3 page width]

Submitted April 4, 2017; accepted Month DD, YYYY

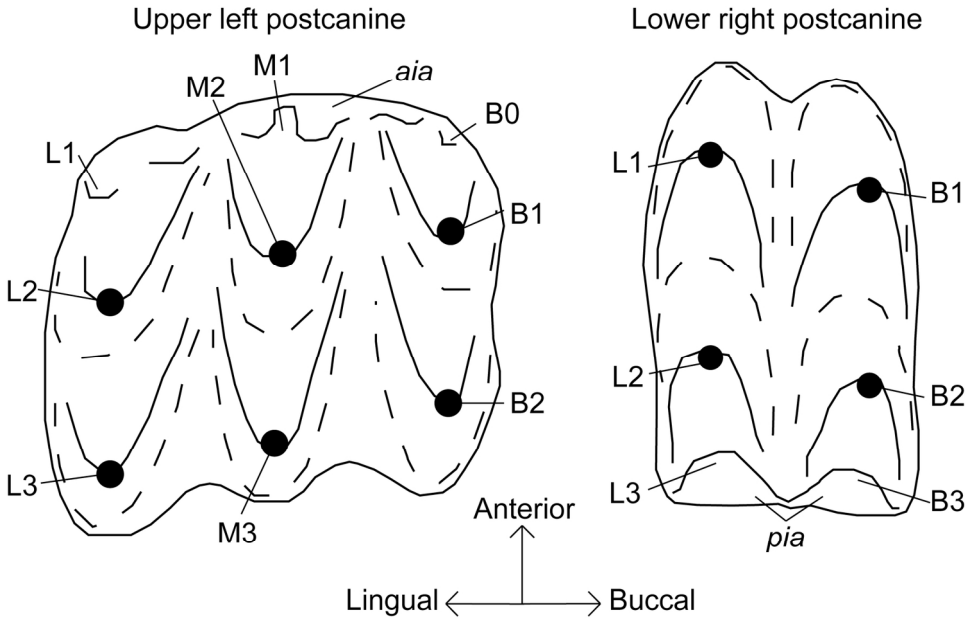

FIGURE 1: Postcanine cusp terminology for *Stereognathus* used in this paper (modified from Watabe et al., 2007). The pia (posterior interlocking area) and aia (anterior interlocking area) are present on both teeth, but the pia is not visible in occlusal view on upper postcanines, and the aia is not visible in occlusal view on lower postcanines, because they are located on the underside of the tooth. [Intended for column width]

78x50mm (600 x 600 DPI)

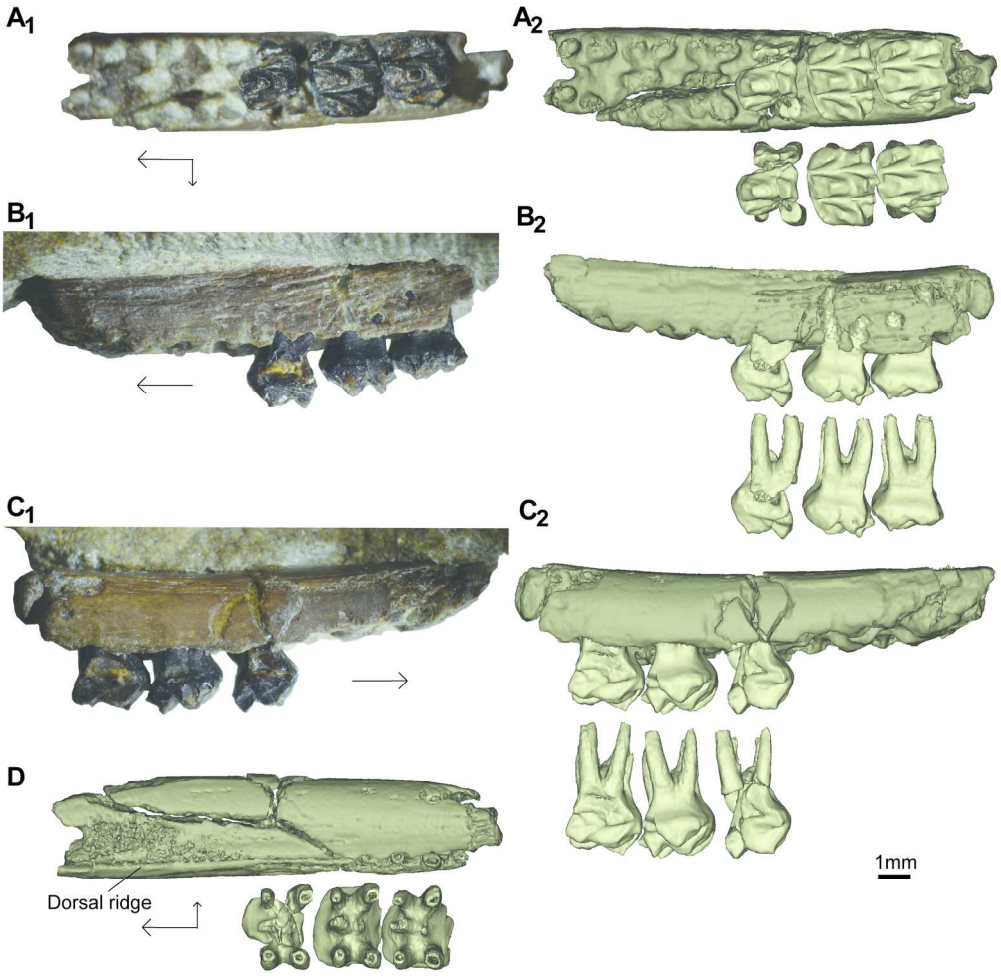

FIGURE 2: *Stereognathus ooliticus* holotype BGS GSM113834. **A1** occlusal view; **A2** occlusal view of CT-scan reconstruction, with teeth segmented from jaw; **B1** buccal view; **B2** buccal view of CT-scan reconstruction, with teeth segmented from jaw; **C1** lingual view; **C2** lingual view of CT-scan reconstruction, with teeth segmented from jaw; **D** dorsal view of maxilla. Anterior direction indicated by longer black arrow, lingual by shorter arrow. [Intended for whole page width]

176x171mm (300 x 300 DPI)

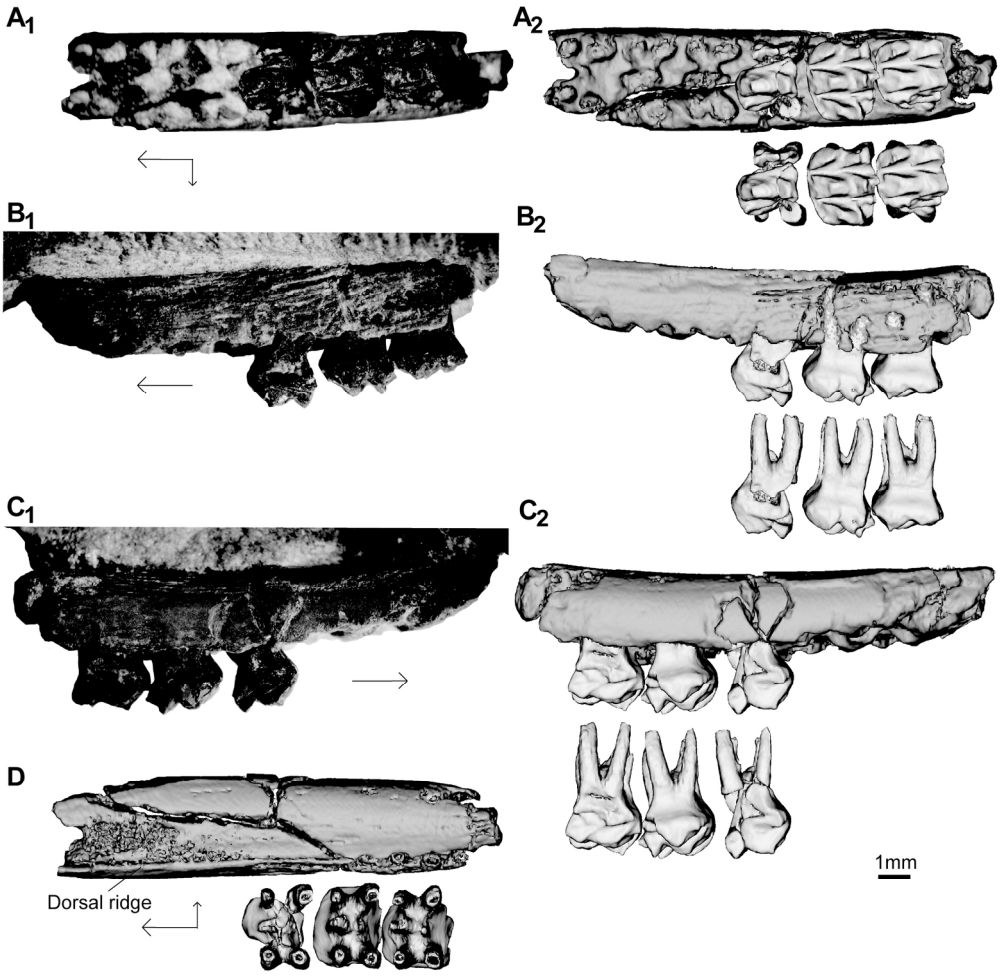

FIGURE 2: *Stereognathus ooliticus* holotype BGS GSM113834. **A1** occlusal view; **A2** occlusal view of CT-scan reconstruction, with teeth segmented from jaw; **B1** buccal view; **B2** buccal view of CT-scan reconstruction, with teeth segmented from jaw; **C1** lingual view; **C2** lingual view of CT-scan reconstruction, with teeth segmented from jaw; **D** dorsal view of maxilla. Anterior direction indicated by longer black arrow, lingual by shorter arrow. [Intended for whole page width]

176x171mm (300 x 300 DPI)

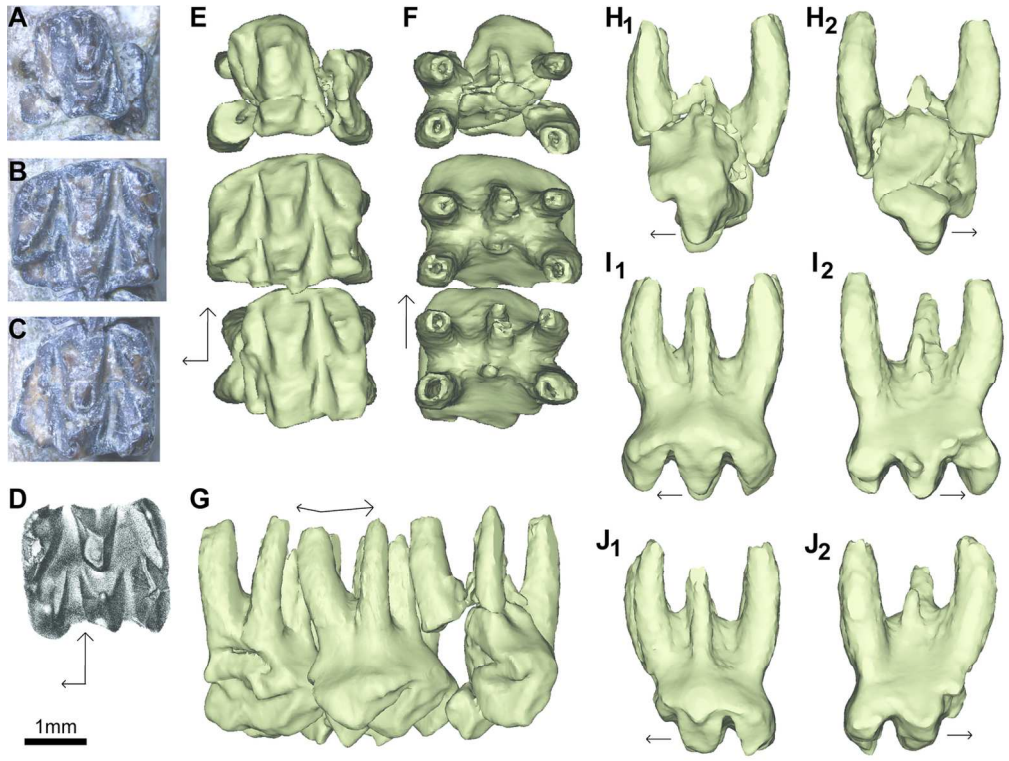

FIGURE 3: *Stereognathus ooliticus* holotype BGS GSM113834, postcanines only. Digitally reconstructed from microCT-scans and segmented from the jaw. **A** occlusal photograph of anteriormost PC; **B** occlusal photograph of middle PC; **C** occlusal photograph of posteriormost PC; **D** original drawing by Owen (1856); **E** occlusal view of digitally reconstructed tooth row: **F** dorsal view of digitally reconstructed tooth row; **G** anterolingual view of digitally reconstructed tooth row; **H1** anterior view of anteriormost PC; **H2** posterior view of anteriormost PC; **I1** anterior view of middle PC; **I2** posterior view of middle PC; **J1** anterior view of posteriormost PC; **J2** posterior view of posteriormost PC. Anterior direction indicated by longer black arrow, lingual by shorter arrow. [Intended for whole page width]

137x103mm (300 x 300 DPI)

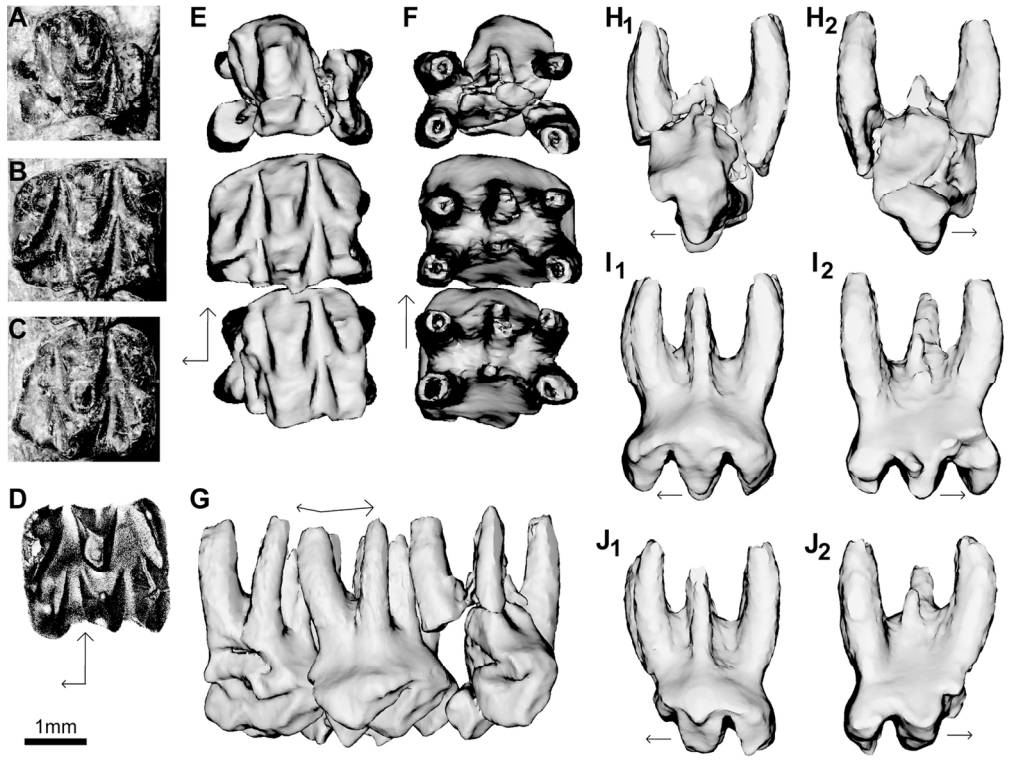

FIGURE 3: *Stereognathus ooliticus* holotype BGS GSM113834, postcanines only. Digitally reconstructed from microCT-scans and segmented from the jaw. **A** occlusal photograph of anteriormost PC; **B** occlusal photograph of middle PC; **C** occlusal photograph of posteriormost PC; **D** original drawing by Owen (1856); **E** occlusal view of digitally reconstructed tooth row: **F** dorsal view of digitally reconstructed tooth row; **G** anterolingual view of digitally reconstructed tooth row; **H1** anterior view of anteriormost PC; **H2** posterior view of anteriormost PC; **I1** anterior view of middle PC; **I2** posterior view of middle PC; **J1** anterior view of posteriormost PC; **J2** posterior view of posteriormost PC. Anterior direction indicated by longer black arrow, lingual by shorter arrow. [Intended for whole page width]

137x103mm (300 x 300 DPI)

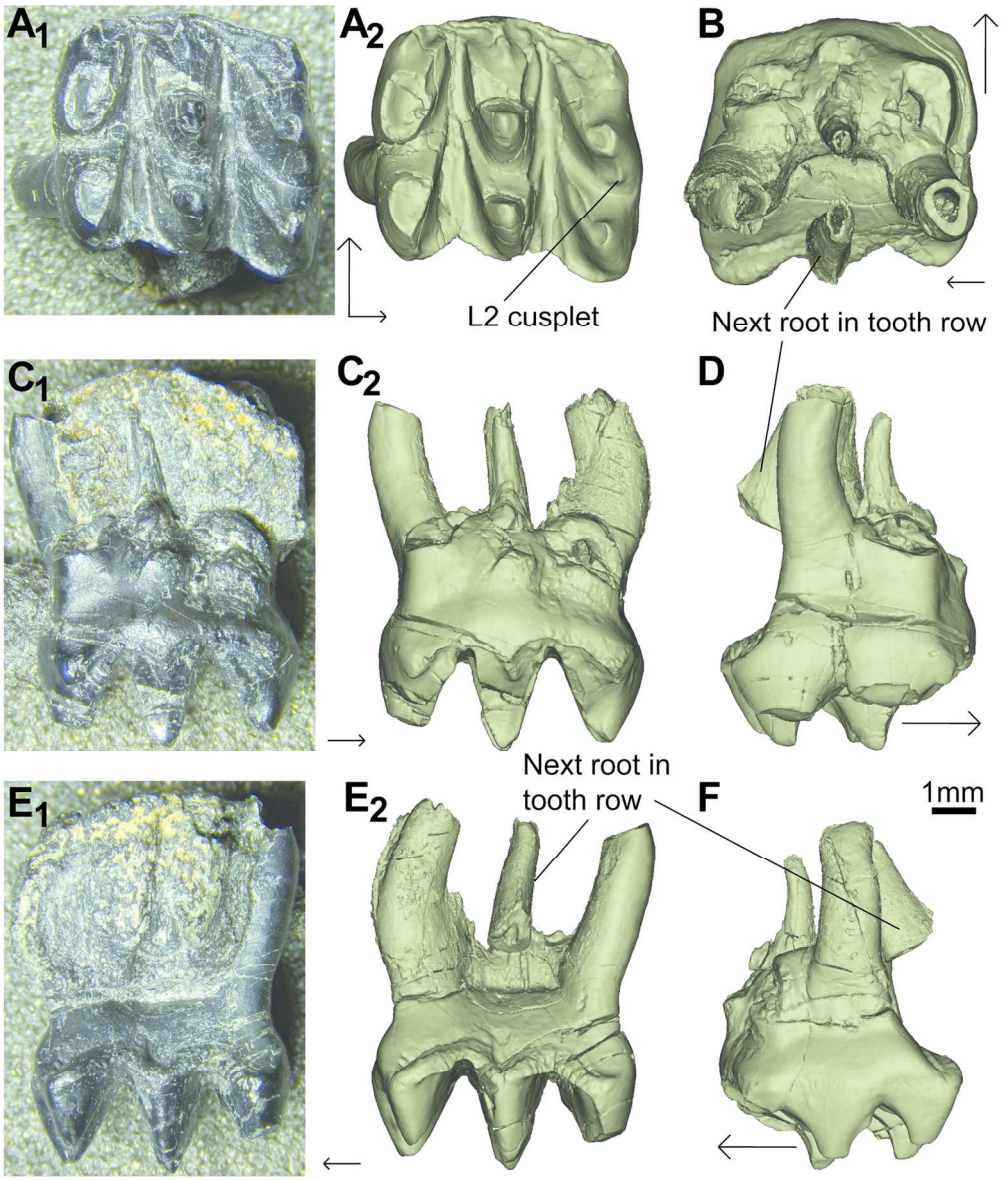

FIGURE 4: Holotype of *Stereognathus hebridicus* BRSUG 20572. **A1** photograph of occlusal surface; **A2** occlusal view from digital reconstruction of CT-scan; **B** dorsal view; **C1** photograph of anterior view; **C2** digital reconstruction of anterior view; **D** buccal view; **E1** photograph of posterior view; **E2** digital reconstruction of posterior view; **F** lingual view. Anterior direction indicated by longer black arrow, lingual by shorter arrow. [Intended for 2/3 page width]

142x167mm (300 x 300 DPI)

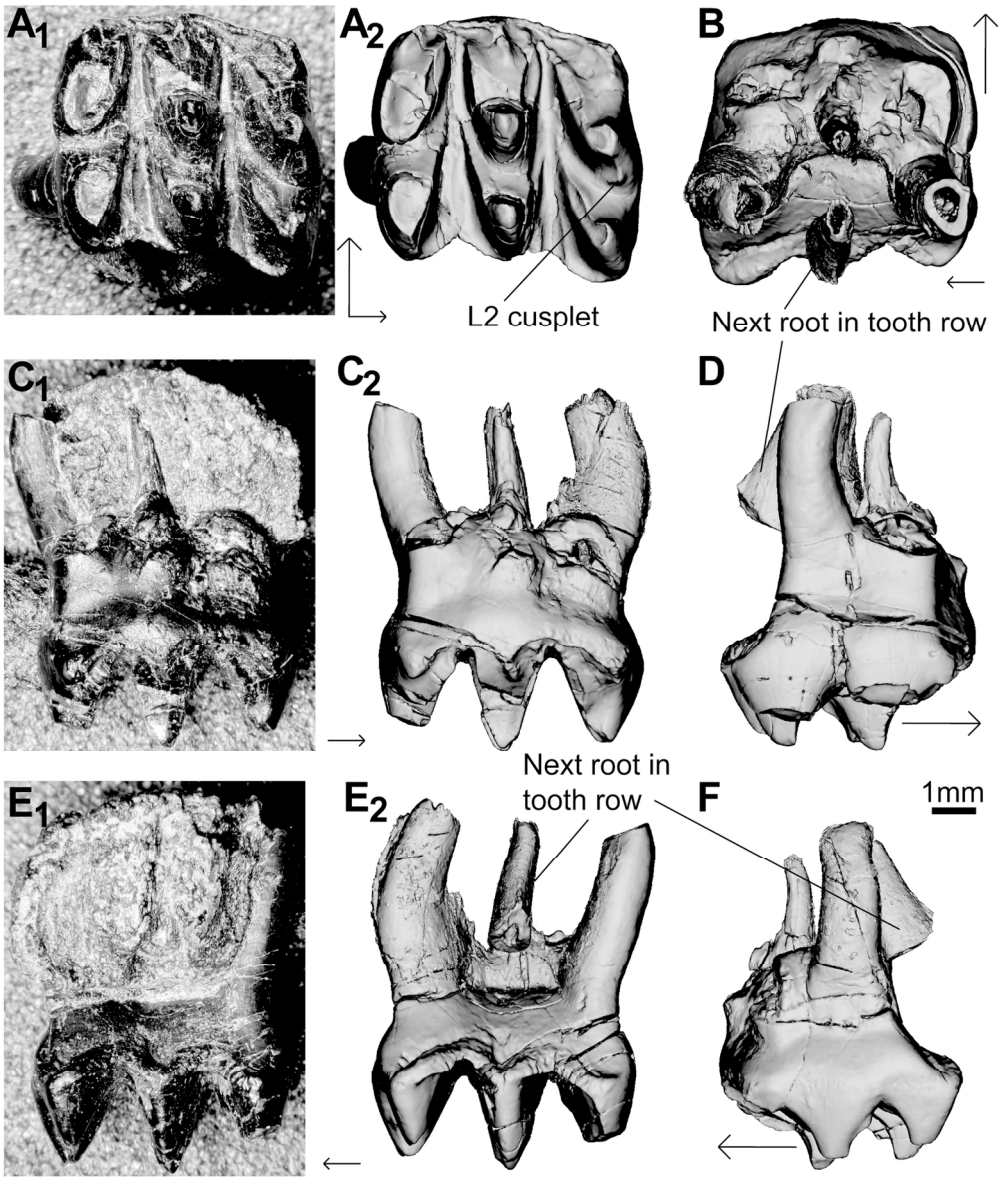

FIGURE 4: Holotype of *Stereognathus hebridicus* BRSUG 20572. **A1** photograph of occlusal surface; **A2** occlusal view from digital reconstruction of CT-scan; **B** dorsal view; **C1** photograph of anterior view; **C2** digital reconstruction of anterior view; **D** buccal view; **E1** photograph of posterior view; **E2** digital reconstruction of posterior view; **F** lingual view. Anterior direction indicated by longer black arrow, lingual by shorter arrow. [Intended for 2/3 page width]

142x167mm (300 x 300 DPI)

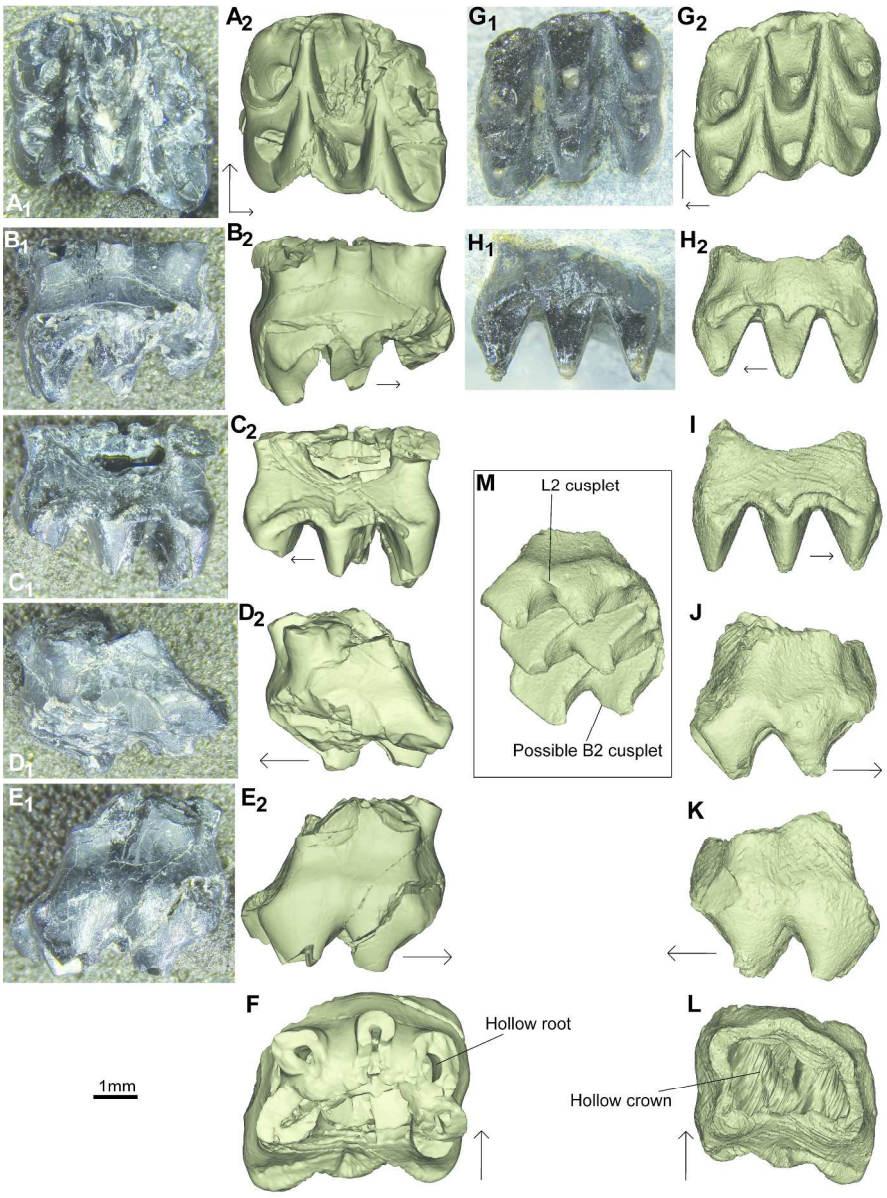

FIGURE 5: Paratype of *Stereognathus hebridicus* upper postcanines BRSUG 20573, and new specimen NMS G.2017.17.2, both reconstructed digitally from CT-scans. **A-F** BRSUG 20573: **A1** occlusal surface; **A2** occlusal surface digital reconstruction; **B1** anterior view; **B2** anterior view digital reconstruction; **C1** posterior view; **C2** posterior view digital reconstruction; **D1** lingual view; **D2** lingual view digital reconstruction; **E1** buccal view; **E2** buccal view digital reconstruction; **F** dorsal view. **G-M** NMS G.2017.17.2: **G1** occlusal surface; **G2** occlusal surface digital reconstruction; **H1** anterior view; **H2** anterior view digital reconstruction; **I** posterior view digital reconstruction; **J** lingual view digital reconstruction; **K** buccal view digital reconstruction; **L** dorsal view; **M** ventrolingual view. Anterior direction indicated by longer black arrow, lingual by shorter arrow. [Intended for whole page width]

246x334mm (300 x 300 DPI)

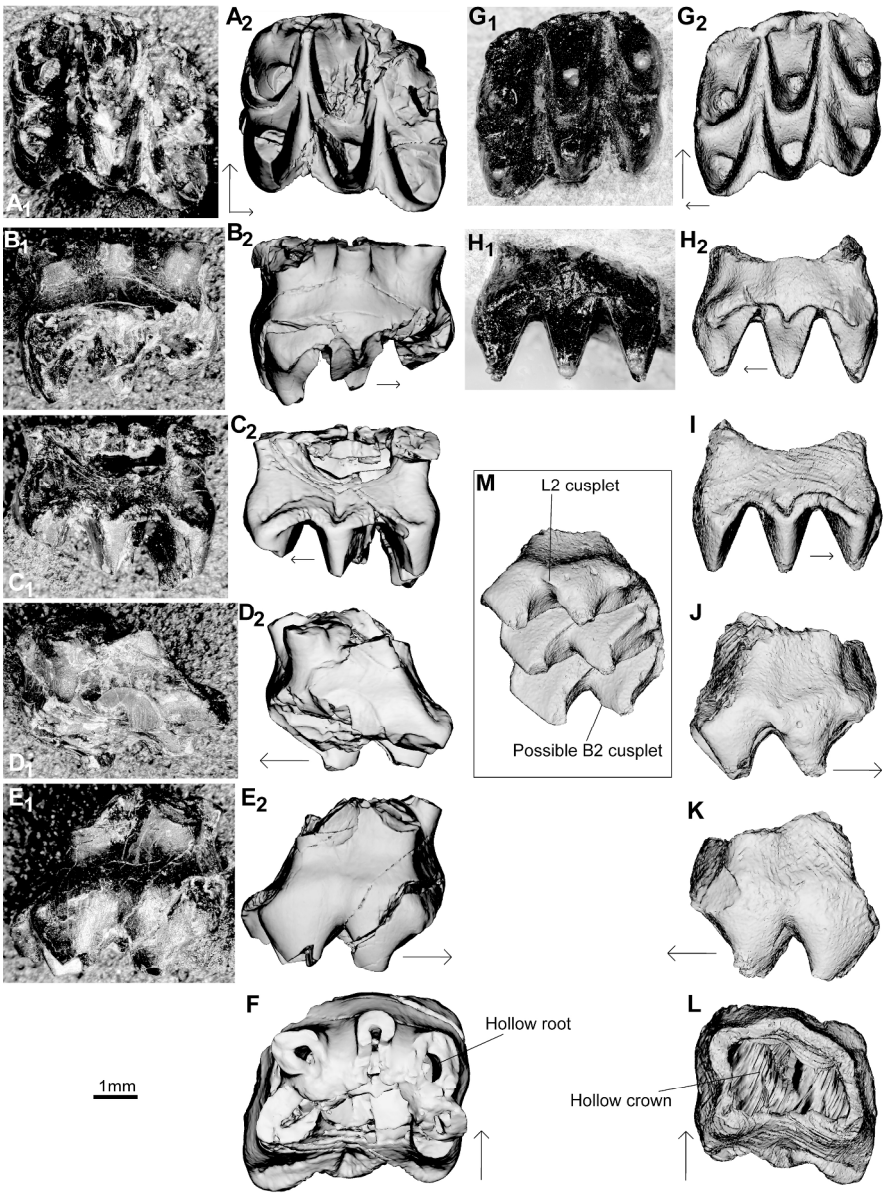

FIGURE 5: Paratype of *Stereognathus hebridicus* upper postcanines BRSUG 20573, and new specimen NMS G.2017.17.2, both reconstructed digitally from CT-scans. **A-F** BRSUG 20573: **A1** occlusal surface; **A2** occlusal surface digital reconstruction; **B1** anterior view; **B2** anterior view digital reconstruction; **C1** posterior view; **C2** posterior view digital reconstruction; **D1** lingual view; **D2** lingual view digital reconstruction; **E1** buccal view; **E2** buccal view digital reconstruction; **F** dorsal view. **G-M** NMS G.2017.17.2: **G1** occlusal surface; **G2** occlusal surface digital reconstruction; **H1** anterior view; **H2** anterior view digital reconstruction; **I** posterior view digital reconstruction; **J** lingual view digital reconstruction; **K** buccal view digital reconstruction; **L** dorsal view; **M** ventrolingual view. Anterior direction indicated by longer black arrow, lingual by shorter arrow. [Intended for whole page width]

246x334mm (300 x 300 DPI)

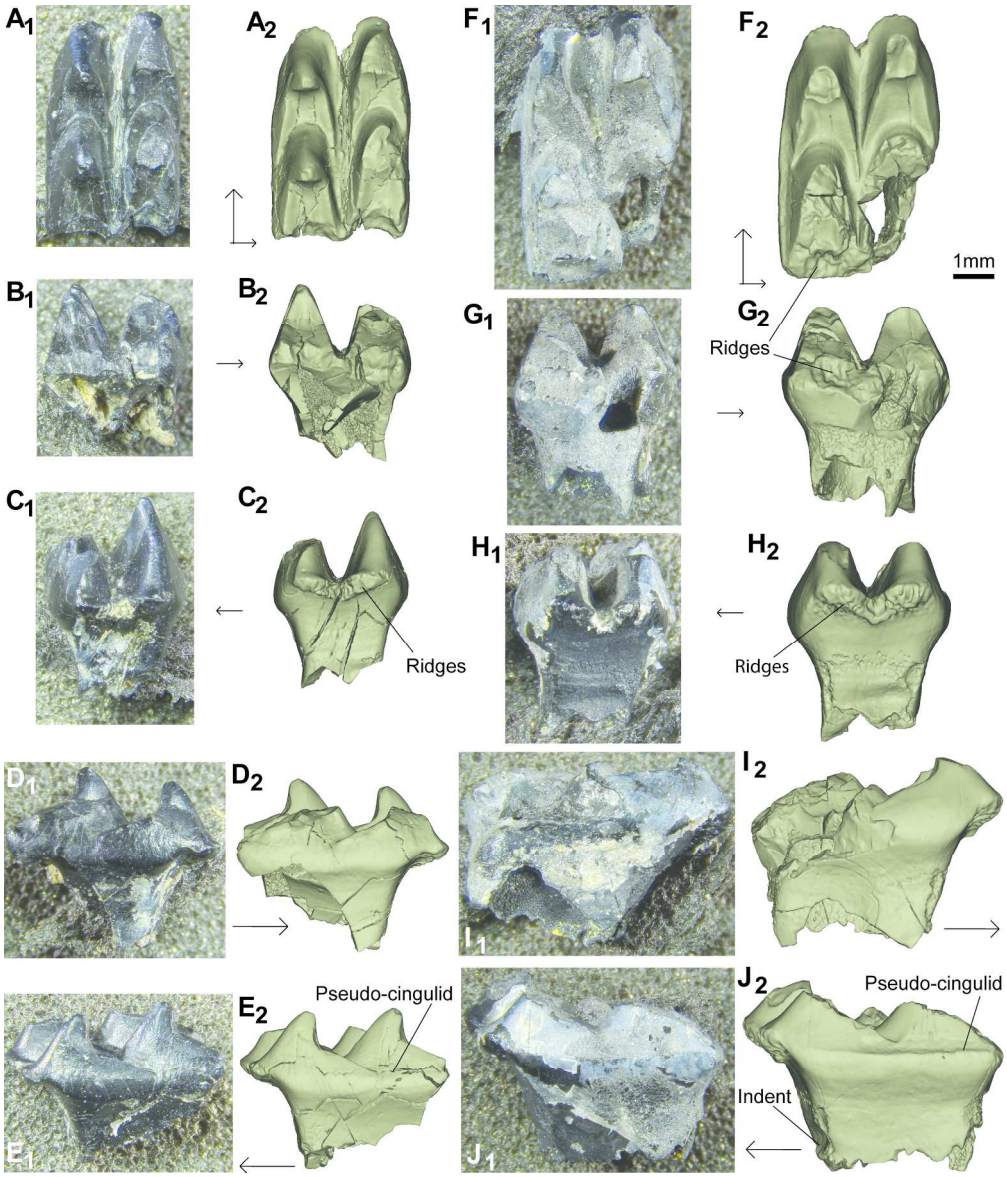

FIGURE 6: Paratypes of *Stereognathus hebridicus* lower postcanines BRSUG 20574 and BRSUG 20575. **A-E** BRSUG 20574: **A1** occlusal view; **A2** occlusal surface digital reconstruction; **B1** posterior view; **B2** posterior view digital reconstruction; **C1** anterior view; **C2** anterior view digital reconstruction; **D1** lingual view; **D2** lingual view digital reconstruction; **E1** buccal view; **E2** buccal view digital reconstruction. **F-J** BRSUG 20575: **F1** occlusal view; **F2** occlusal surface digital reconstruction; **G1** posterior view; **G2** posterior view digital reconstruction; **H1** anterior view; **H2** anterior view digital reconstruction; **I1** lingual view; **I2** lingual view digital reconstruction; **J1** buccal view; **J2** buccal view digital reconstruction. Anterior direction indicated by longer black arrow, lingual by shorter arrow. [Intended for whole page width]

212x247mm (300 x 300 DPI)

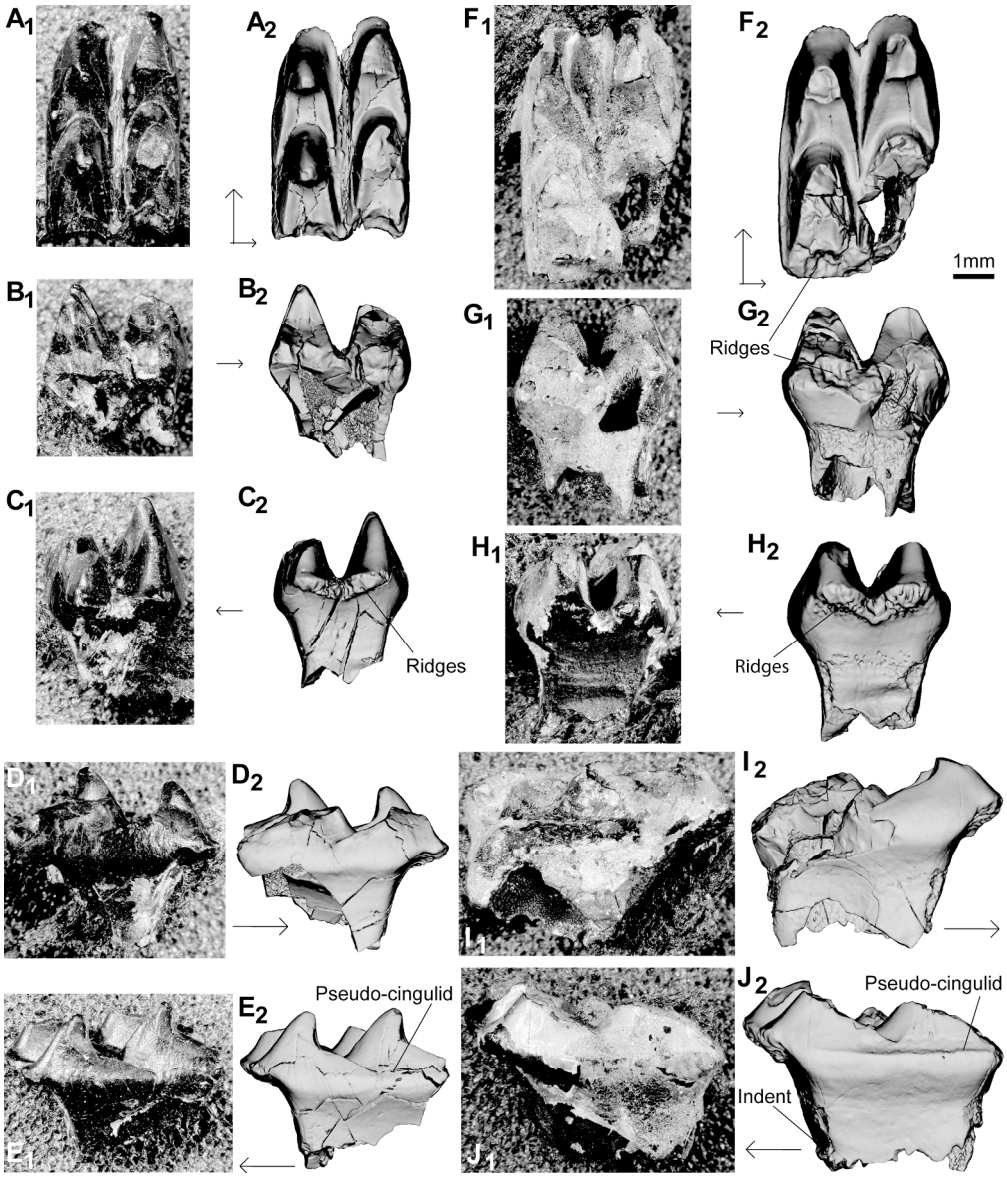

FIGURE 6: Paratypes of *Stereognathus hebridicus* lower postcanines BRSUG 20574 and BRSUG 20575. **A-E** BRSUG 20574: **A1** occlusal view; **A2** occlusal surface digital reconstruction; **B1** posterior view; **B2** posterior view digital reconstruction; **C1** anterior view; **C2** anterior view digital reconstruction; **D1** lingual view; **D2** lingual view digital reconstruction; **E1** buccal view; **E2** buccal view digital reconstruction. **F-J** BRSUG 20575: **F1** occlusal view; **F2** occlusal surface digital reconstruction; **G1** posterior view; **G2** posterior view digital reconstruction; **H1** anterior view; **H2** anterior view digital reconstruction; **I1** lingual view; **I2** lingual view digital reconstruction; **J1** buccal view; **J2** buccal view digital reconstruction. Anterior direction indicated by longer black arrow, lingual by shorter arrow. [Intended for whole page width]

212x247mm (300 x 300 DPI)

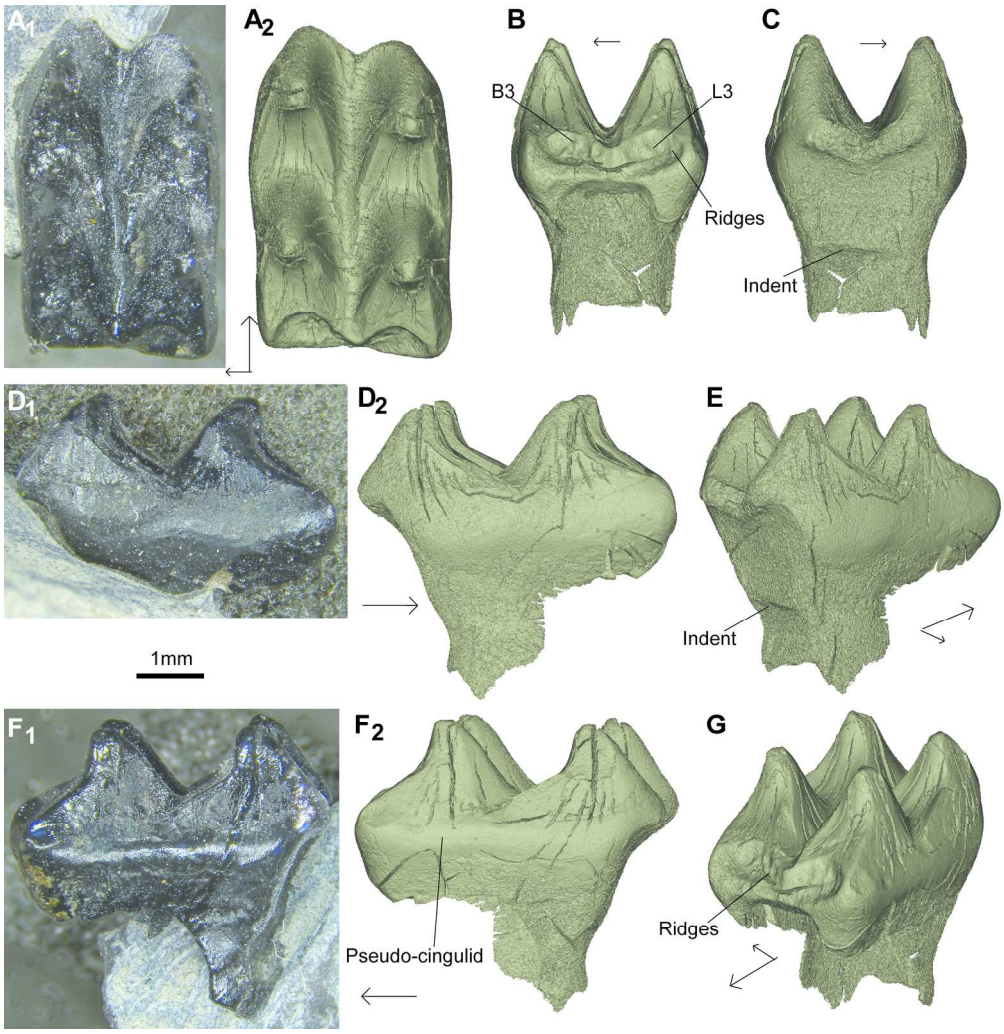

FIGURE 7: New specimen NMS G.1992.47.120, a lower postcanine reconstructed digitally from CT-scans. **A1** occlusal surface; **A2** occlusal surface digital reconstruction; **B** posterior view reconstruction; **C** anterior view digital reconstruction; **D1** lingual view; **D2** lingual view digital reconstruction; **E** anterolingual view; **F1** buccal view; **F2** buccal view digital reconstruction; **G** posterobuccal view. Anterior direction indicated by longer black arrow, lingual by shorter arrow. [Intended for whole page width]

186x190mm (300 x 300 DPI)

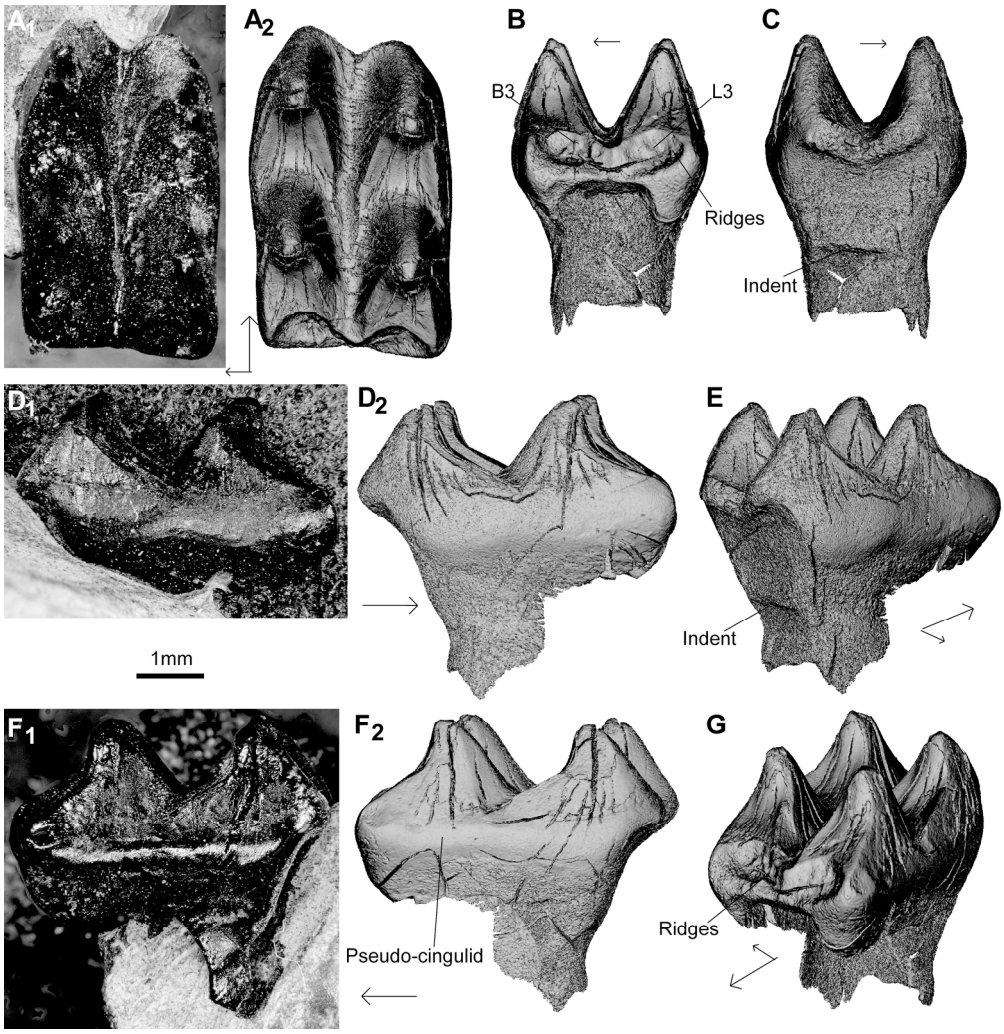

FIGURE 7: New specimen NMS G.1992.47.120, a lower postcanine reconstructed digitally from CT-scans. **A1** occlusal surface; **A2** occlusal surface digital reconstruction; **B** posterior view reconstruction; **C** anterior view digital reconstruction; **D1** lingual view; **D2** lingual view digital reconstruction; **E** anterolingual view; **F1** buccal view; **F2** buccal view digital reconstruction; **G** posterobuccal view. Anterior direction indicated by longer black arrow, lingual by shorter arrow. [Intended for whole page width]

186x190mm (300 x 300 DPI)

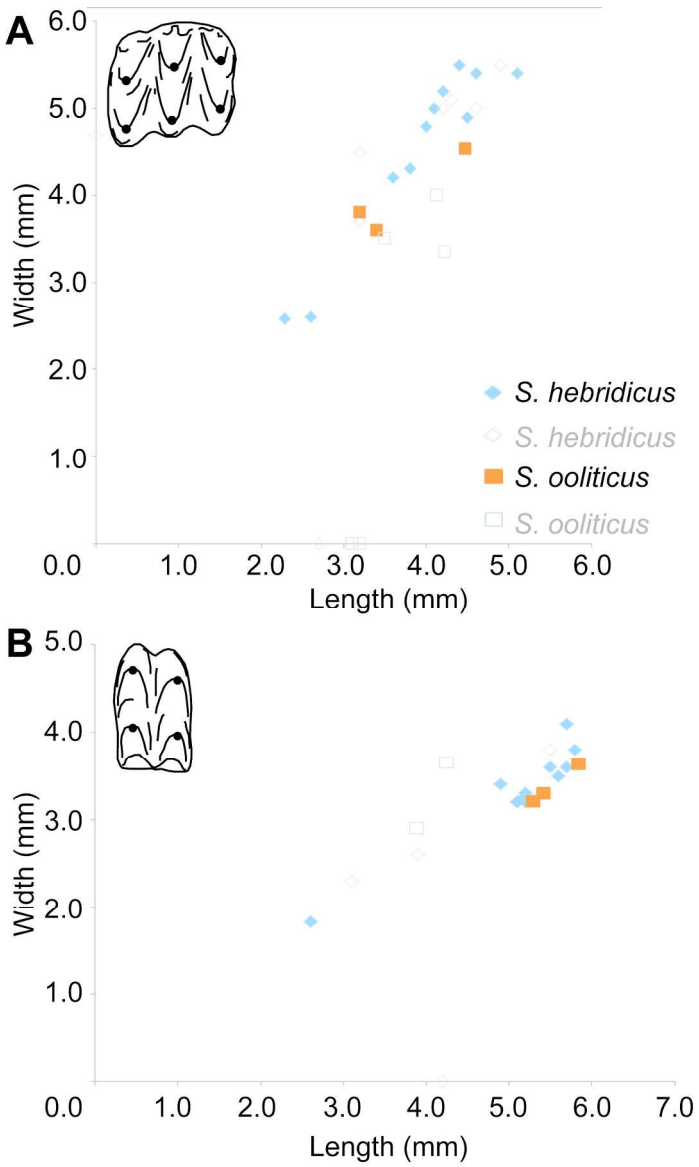

FIGURE 8: Scatterplots of postcanine measurements of *Stereognathus*. **A** shows upper postcanines, **B** shows lower postcanines. Key for **B**, as in **A**. Complete specimens are filled shapes (orange square = *S. ooliticus*, blue diamond = *S. hebridicus*) incomplete are not filled. Measurements in Table 1. [Intended for column width]

151x257mm (300 x 300 DPI)

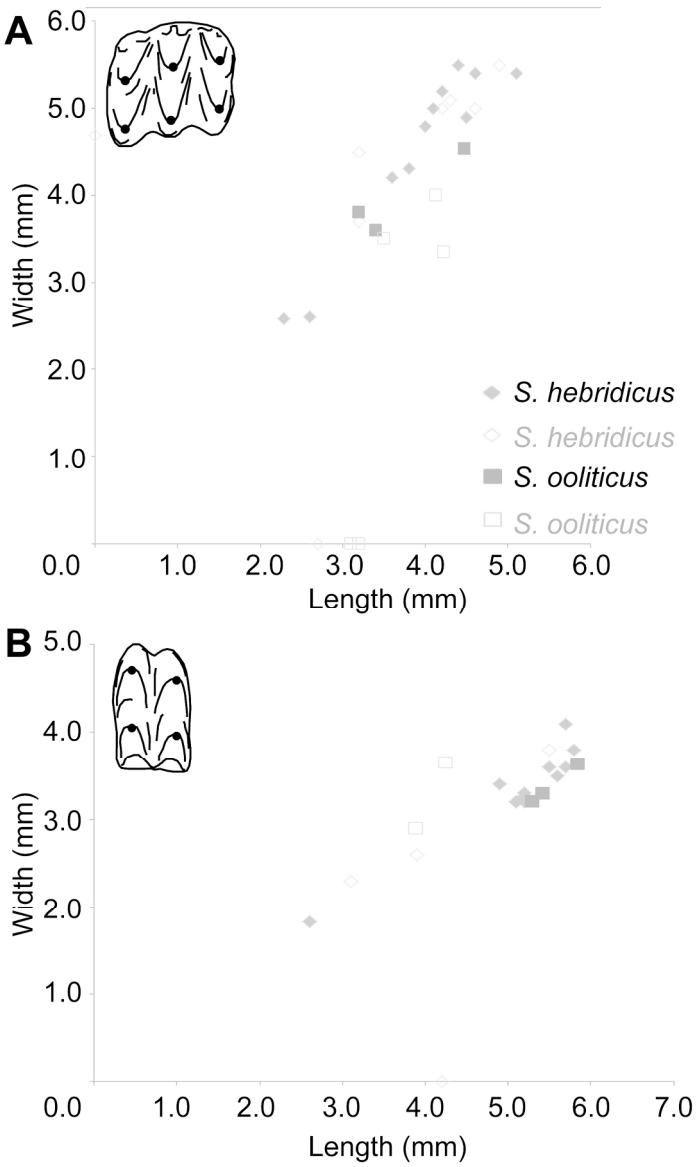

FIGURE 8: Scatterplots of postcanine measurements of *Stereognathus*. **A** shows upper postcanines, **B** shows lower postcanines. Key for **B**, as in **A**. Complete specimens are filled shapes (orange square = *S. ooliticus*, blue diamond = *S. hebridicus*) incomplete are not filled. Measurements in Table 1. [Intended for column width]

151x257mm (300 x 300 DPI)

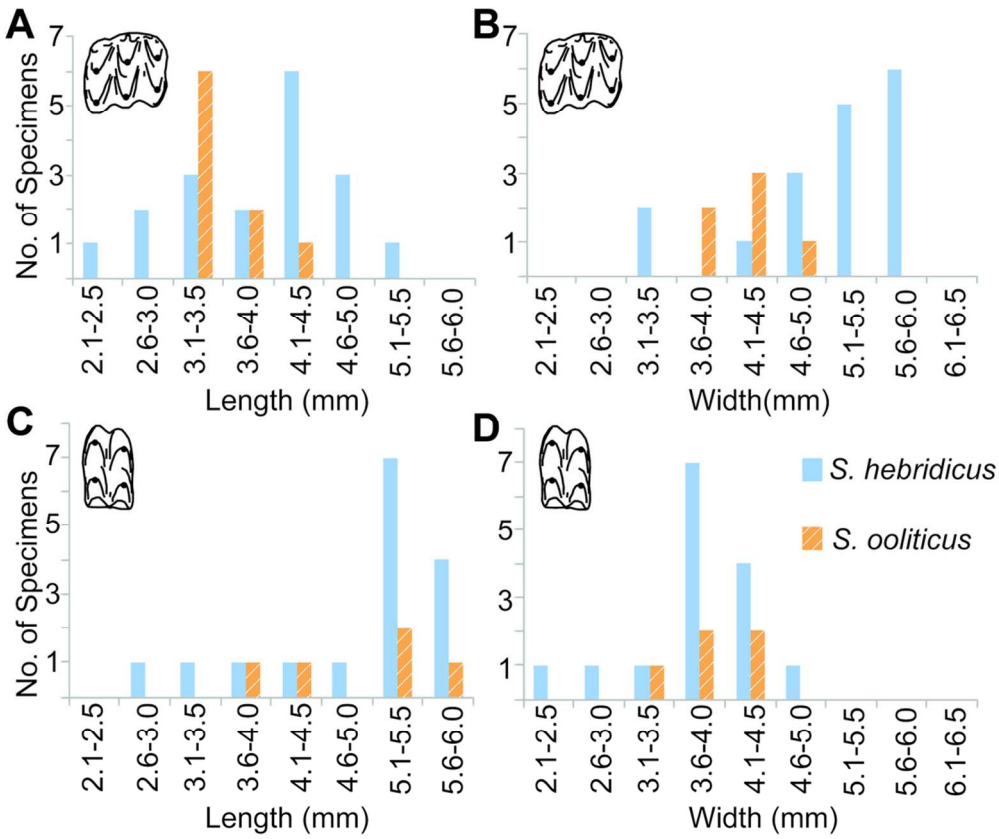

FIGURE 9: Distribution of *Stereognathus* postcanine specimens. **A** is upper PC length, **B** is upper PC width, **C** is lower pc length, **D** is lower pc width. Orange striped = *S. ooliticus*, blue non-striped = *S. hebridicus*. [Intended for 2/3 page width]

100x83mm (300 x 300 DPI)

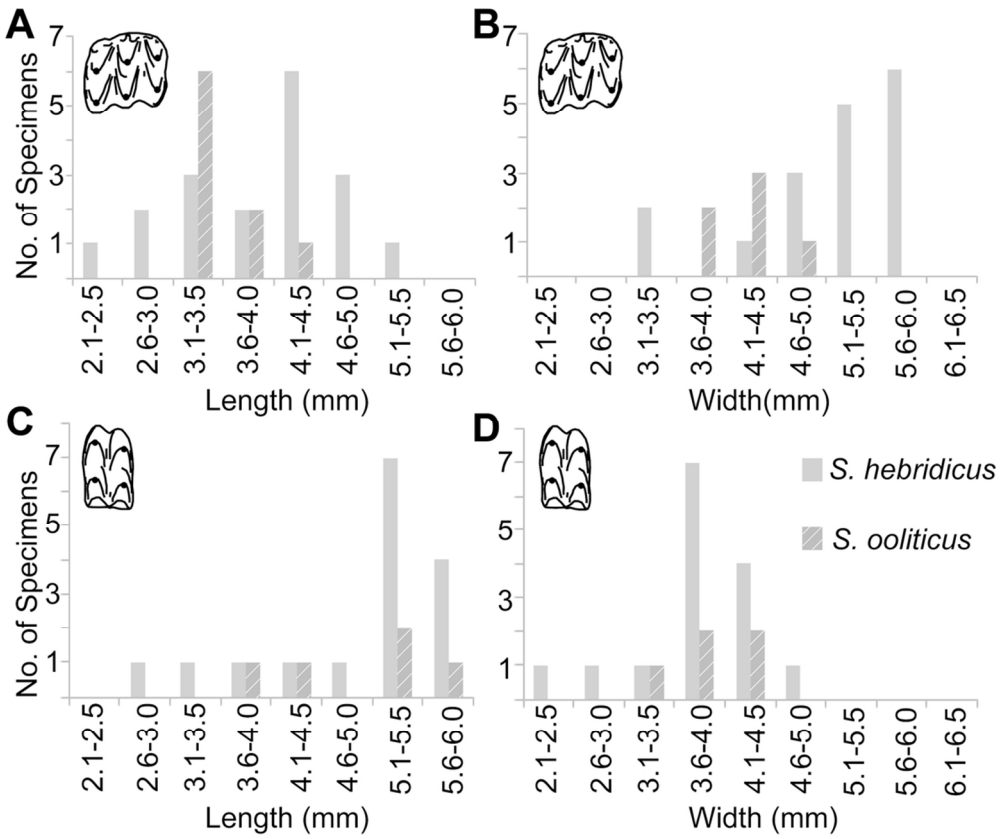

FIGURE 9: Distribution of *Stereognathus* postcanine specimens. **A** is upper PC length, **B** is upper PC width, **C** is lower pc length, **D** is lower pc width. Orange striped = *S. ooliticus*, blue non-striped = *S. hebridicus*. [Intended for 2/3 page width]

100x83mm (300 x 300 DPI)

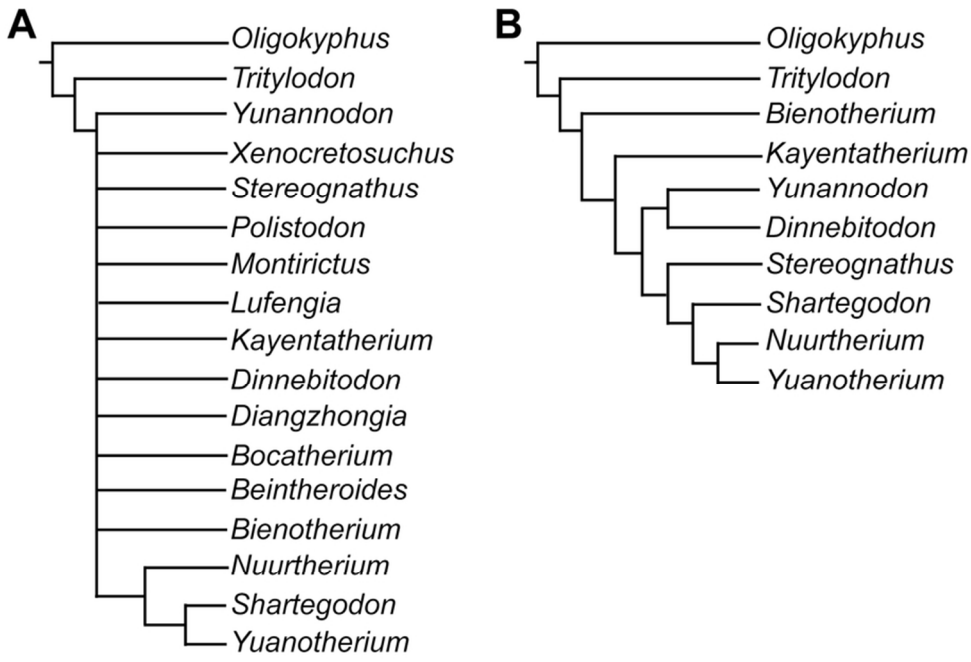

FIGURE 10: Trees generated by our phylogenetic analysis of tritylodontid taxa, using updated characters for *Stereognathus*. **A** is the strict consensus of the five parsimonious trees of 71 steps. **B** is the agreement subtree of 10 taxa. [Intended for 2/3 page width]

80x52mm (300 x 300 DPI)

TABLE 1: Measurements of UK *Stereognathus* material. Measurements where slight breakages or wear made measurement uncertain (estimated measurements referred to in text) are in italics, and underlined where breakage was more significant.

Specimen No.	Species	Locality	Description	Length (mm)	Width (mm)	Width/ Length
BRSUG 20572	*hebridicus*		Holotype upper	5.1	5.4	1.06
BRSUG 20573	*hebridicus*	Kilmaluag	Paratype upper	4.8	5.4	1.13
BRSUG 20574	*hebridicus*	Kilmaluag	Paratype lower right	5.1	3.2	0.63
BRSUG 20575	*hebridicus*	Kilmaluag	Paratype lower right	5.8	3.8	0.66
BRSUG 29000	*hebridicus*	Kilmaluag, Skye	Fragmentary: upper left molar	NA	4.7	-
			Fragmentary:: lower molar	*3.1*	*2.3*	0.74
			Fragmentary:	NA	3.5	-

TABLE 1. (Continued)

			cusps			
BRSUG 29002	*hebridicus*	Kilmaluag	Upper right	3.6	NA	-
BRSUG 28996_A	*hebridicus*	Kilmaluag	Upper right	4.5	4.9	1.09
BRSUG 28996_B	*hebridicus*	Kilmaluag	Upper left	4.2	5.2	1.24
BRSUG 28996_C	*hebridicus*	Kilmaluag	Upper right	4.4	5.5	1.25
BRSUG 28996_D	*hebridicus*	Kilmaluag	Upper right	2.3	2.6	1.13
BRSUG 28996_E	*hebridicus*	Kilmaluag	Upper right	*4.3*	*5.1*	1.19
BRSUG 28997_A	*hebridicus*	Kilmaluag	Upper	*3.2*	3.7	1.16
BRSUG 28997_B	*hebridicus*	Kilmaluag	Upper	4.1	5.0	1.22
BRSUG 28997_C	*hebridicus*	Kilmaluag	Upper	*4.2*	*5.0*	1.19
BRSUG 28997_D	*hebridicus*	Kilmaluag	Upper	4.9	5.5	1.12

TABLE 1. (Continued)

BRSUG 28997_E	*hebridicus*	Kilmaluag	Upper	2.6	2.6	1.00
BRSUG 28997_F	*hebridicus*	Kilmaluag	Upper	3.6	4.2	1.17
BRSUG 28997_G	*hebridicus*	Kilmaluag	Upper	4.0	4.8	1.20
BRSUG 28998_A	*hebridicus*	Kilmaluag	Lower	5.5	3.6	0.65
BRSUG 28998_B	*hebridicus*	Kilmaluag	Lower	5.6	3.5	0.63
BRSUG 28998_C	*hebridicus*	Kilmaluag	Lower	*4.9*	3.4	0.69
BRSUG 28998_D	*hebridicus*	Kilmaluag	Lower	5.2	3.2	0.62
BRSUG 28998_E	*hebridicus*	Kilmaluag	Lower	5.2	3.3	0.63
BRSUG 28998_F	*hebridicus*	Kilmaluag	Upper	4.6	5.0	1.09
BRSUG 28999_A	*hebridicus*	Kilmaluag	Lower	5.2	3.3	0.63

TABLE 1. (Continued)

BRSUG 28999_B	*hebridicus*	Kilmaluag	Lower	5.1	3.2	0.63
BRSUG 28999_C	*hebridicus*	Kilmaluag	Lower	3.9	2.6	0.67
BRSUG 28999_D	*hebridicus*	Kilmaluag	Lower	2.6	1.8	0.69
BRSUG 28999_E	*hebridicus*	Kilmaluag	Upper fragment	2.7	NA	-
NMS G.1992.47.120	*hebridicus*	Kilmaluag	Lower	5.7	3.6	0.63
NMS G.2017.17.1	*hebridicus*	Kilmaluag	Lower	4.2	NA	
NMS G.2017.17.2	*hebridicus*	Kilmaluag	Upper	3.8	4.3	1.13
NMS G.2017.17.3	*hebridicus*	Kilmaluag	Lower	*5.5*	3.8	0.69
NMS G.2017.17.4	*hebridicus*	Kilmaluag	Upper fragmented	*3.2*	*4.5*	1.41
NMS G.2017.17.5	*hebridicus*	Kilmaluag	lower	NA	3.6	

TABLE 1. (Continued)

NMS G.2017.17.6	*hebridicus*	Kilmaluag	Lower	5.7	4.1	0.72
BGS GSM113834	*ooliticus*	Stonesfield	Jaw fragment with 3PCs: anterior	*3.1*	NA	-
	ooliticus	Stonesfield	middle	3.4	3.6	1.06
	ooliticus	Stonesfield	posterior	3.5	*3.5*	1.00
GLRCM - G75710-ulm	*ooliticus*	Hornsleasow	Upper	4.5	4.5	1.02
GLRCM _MLR_20-22	*ooliticus*	Hornsleasow	Upper	4.2	*3.4*	0.79
GLRCM _MLR_20-38	*ooliticus*	Hornsleasow	Upper	*4.1*	*4.0*	0.97
GLRCM _H174	*ooliticus*	Hornsleasow	Lower	5.8	3.6	0.62
GLRCM TEMP2105_4	*ooliticus*	Hornsleasow	Lower	*4.3*	3.7	0.86
GLRCM TEMP2105_6	*ooliticus*	Hornsleasow	Lower	*3.9*	2.9	0.74

TABLE 1. (Continued)

OUMNH J.79435	*ooliticus*	Kirtlington	Upper	3.1	NA	-
OUMNH J.79439	*ooliticus*	Kirtlington	Lower	3.2	NA	-
OUMNH J.79480	*ooliticus*	Kirtlington	Upper	3.2	3.8	1.19
DORCM G 11048	*ooliticus*	Forest Marble	Lower	5.3	3.2	0.60
DORCM G10828-lrm	*ooliticus*	Forest Marble	Lower	5.4	3.3	0.61

TABLE 2: The dataset used for analysis, including estimated measurements.

	S. ooliticus				*S. hebridicus*			
	Uppers		Lowers		Uppers		Lowers	
	length	width	length	width	length	width	length	width
Mean	3.59	3.80	4.94	3.33	3.91	4.63	4.89	3.25
sample size	9.00	5.00	5.00	5.00	19.00	15.00	16.00	15.00
sample range	1.37	1.20	1.95	0.75	2.81	2.90	3.20	2.27
s2	0.10	0.23	0.69	0.10	0.62	0.95	0.91	0.36
s	0.32	0.48	0.83	0.31	0.79	0.97	0.95	0.60

APPENDIX 1. Description of characters in phylogenetic analysis

Characters and scorings are from Velazco et al. (2017), except *Stereognathus*, which was rescored based on our updated morphological description. Characters are unordered. *Oligokyphus* is the outgroup.

(1) Snout: longer than postcanine toothrow length (0); shorter than postcanine toothrow length (1).

(2) Postincisive constriction of the snout: present (0); absent (1).

(3) Anterior margin of orbit: directly dorsal to the distal margin of PC1 (0); above the anteroposterior midpoint of PC2 (1).

(4) Lacrimal size: large (0); reduced (1).

(5) Lacrimal foramina: absent (0); one (1); two (2).

(6) Anterior contact of lacrimal: premaxilla (0); maxilla (1).

(7) Premaxilla posterior extension on secondary palate: anteriorly (0); between incisors and the mesial cheek teeth (1); near the most mesial teeth (2).

(8) Contact between premaxilla and palatine on palate: absent (0); present (1).

(9) Premaxilla-maxillary: contact follows the mesiolingual shape of PC1 (0); contact occurs in the snout (1).

(10) Interdigitations on the maxillo-palatine suture: absent (0); present (1).

(11) Interdigitations on the premaxillo-palatine suture: absent (0); present (1).

(12) Maxilla presence on the hard palate: large and occupies most of the area of the palate (0); highly reduced, preserved as a narrow band forming the lingual margins of the postcanine teeth (1).

APPENDIX 1. (Continued)||

(13) Palatine contact: anteriorly and laterally, the palatine is bordered by the maxilla and premaxilla (0); bordered only by the maxilla (1).

(14) Palatine contribution to the PC4 alveolus: present (0); absent (1).

(15) Greater palatine foramina: three (0); two (1); one (2); absent (3).

(16) Lateral (facial and zygomatic) extension of maxilla: present (0); reduced or absent (1).

(17) Zygomatic process of the maxilla: constitutes the ventral aspect of the anterior root of the zygomatic arch (0); constitutes the dorsal aspect of the anterior root of the zygomatic arch (1).

(18) Jugal contribution to the medial and inferior orbital walls: present (0); absent (1).

(19) Foramina on jugal above PC2: three foramina present (0); absent (1).

(20) Coronoid process height: very tall (0); short (1).

(21) Coronoid process anterior margin shape: gently curved anterior margin (0); straight anterior margin (1).

(22) Angle of the alveolar line and the anterior margin of the coronoid process: <90º (0); >90º (1); 90º (2).

(23) Upper postcanine alveolar tooth rows: diverge posteriorly (0); parallel (1).

(24) Upper postcanine teeth generalize cusp formula: 2-2-2 (0); 2-3-2 (1); 2-3-3 (2); 2-3-4 (3); 2-4-3 (4); 2-4-4 (5); 3-3-3 (6); 3-4-4 (7).

(25) Upper cheek tooth B0 cusp: present (0); absent (1).

(26) Upper cheek tooth M0 cusp: present (0); absent (1).

APPENDIX 1. (Continued)||

(27) Upper cheek tooth L0 cusp: present (0); absent (1).

(28) Upper cheek tooth M1 cusp: large (0); small (1); absent (2).

(29) Upper cheek tooth L1 cusp: large (0); small (1); absent (2).

(30) Upper cheek tooth L3 cusp: large (0); small (1); absent (2).

(31) Upper postcanine roots: four (0); five (1); six (2); seven (3).

(32) Upper postcanine teeth anterior median root: absent (0); present (1).

(33) Lower postcanine teeth generalize cusp formula: 2-2 (0); 3-3 (1).

(34) Lower postcanine root number: one (0); two (1).

(35) Lower postcanine root length and curvature: long with the distal 2/3 curved (0); long and curved throughout its entire length (1); short and slightly curved (2).

APPENDIX 2. Character matrix used for phylogenetic analysis.

Polymorphisms are as follows: A, (0.2), B (2,6), C (1,0) D (2,3).

Taxon	10	20	30	35
Bienotherium	1100111011	-011200???	??02111010	21?11
Bienotherium	1110102100	1101A1????	??0BC11110	10000
Bocatherium	1100102100	110111???0	0210111220	?????
Dianzhongia	11????20??	?????0????	??11111001	3????
Dinnebitodon	11????21??	?1???1????	??01111002	?????
Kayentatherium	1100112001	-0?1200110	0002111010	??0??
Lufengia	11????20??	?????0????	???2111000	10?12
Montirictus	??????????	??????????	???0111220	20011
Oligokyphus	0000210011	-011300111	1107000000	21111
Polistodon	11?101????	?????000?1	01?0111220	??0??
Stereognathus	??????????	?1?1?1????	???0011110	D10?0
Tritylodon	00???10011	-011200??0	0212111000	11???
Xenocretosuchus	??????????	??????????	???0111220	??0??
Yunnanodon	11????????	??????????	???1111002	10?12
Yuanotherium	??????2100	11??101???	???4000011	?????
Shartegodon	1100?02100	0100100000	??05100110	00000
Nuurtherium	?????????0	?1????????0	0003100010	10000